

## MASTER

### Eddy Current field compensation design and implementation of a control system in MRI systems

Derksen, H.B.G.

*Award date:*  
1999

[Link to publication](#)

#### **Disclaimer**

This document contains a student thesis (bachelor's or master's), as authored by a student at Eindhoven University of Technology. Student theses are made available in the TU/e repository upon obtaining the required degree. The grade received is not published on the document as presented in the repository. The required complexity or quality of research of student theses may vary by program, and the required minimum study period may vary in duration.

#### **General rights**

Copyright and moral rights for the publications made accessible in the public portal are retained by the authors and/or other copyright owners and it is a condition of accessing publications that users recognise and abide by the legal requirements associated with these rights.

- Users may download and print one copy of any publication from the public portal for the purpose of private study or research.
- You may not further distribute the material or use it for any profit-making activity or commercial gain

#### **Take down policy**

If you believe that this document breaches copyright please contact us providing details, and we will remove access to the work immediately and investigate your claim.

# Eddy Current Field Compensation

Design and Implementation of a  
Control System in MRI systems

by H.B.G. Derksen

Master of Science thesis  
July 1998 – April 1999

Under supervision of: Prof. dr. ir. P.P.J. van den Bosch  
Coached by: ir. V. van Acht, ir. D. de Bruin, ir. W. van Groningen, ing. A.  
Machielsen

# Abstract

Concluding the Master of Science study in Electrical Engineering at the Eindhoven University of Technology, this Master project has been carried out in association with Philips Medical Systems.

Subject of the project is to study the possibility of designing and implementing a control system to automate the compensation of Eddy Current fields in an MRI system. Eddy Current fields are induced in MRI systems due to pulsed magnetic field gradients. Compensation is done by pre-emphasising the current which induces the desired gradient field. This pre-emphasis is totally described by the Eddy Current influences on the magnetic gradient field.

Two methods have been studied to identify the Eddy Current influences. One includes system knowledge: compact system identification, the other does not include system knowledge: black-box system identification. Compact system identification requires a model for the Eddy Current field. This model is identified in continuous time. The black-box identification is a discrete time identification, the model is dictated by the chosen black-box identification (e.g. Output Error, Box Jenkins, Steiglitz-McBride, etc.) For both methods computer simulations have been done on real measurement data. This gave very satisfying results.

Compact system identification has been implemented and tested. This resulted in compensation of the Eddy Current field within system requirements. Black-box identification has the advantage that no a priori knowledge of the system is needed, especially for future developments in the MRI systems. Implementations can vary from a software implementation or the use of a DSP to a total hardware implementation. The test of the compact system identification was done using a DSP.

Main result is that a control system can be used to automate the compensation of Eddy Current fields. Black-box identification appears to have the advantage for future developments, so it is recommended to further study and test this method.

# Contents

<b>Abstract .....</b>	<b>i</b>
<b>Contents .....</b>	<b>ii</b>
<b>List of Abbreviations .....</b>	<b>iv</b>
<b>1 Introduction .....</b>	<b>1</b>
1.1 Measuring the Gradient Field Response .....	2
1.2 Manual Eddy Current Compensation .....	3
1.2.1 Step Response Model in Short .....	3
1.2.2 Compensation Procedure .....	4
1.3 Automated Eddy Current Compensation .....	6
<b>2 Compact System Identification .....</b>	<b>7</b>
2.1 Introduction .....	7
2.2 Model for System Identification .....	7
2.2.1 Modelling with Electric Circuits .....	7
2.2.2 Model Restrictions .....	9
2.2.3 Fitting the Step Response .....	9
2.2.4 Single Shot Step Response .....	10
2.2.5 Multi Shot Step Response .....	12
2.3 System Identification & Compensation .....	12
2.3.1 Algorithm .....	12
2.3.2 Step to Ramp Response .....	14
2.3.3 System Parameters .....	15
Compensation .....	18
2.4 Conclusion .....	19
<b>3 Black-Box System Identification &amp; Compensation .....</b>	<b>21</b>
3.1 Introduction .....	21
3.2 Steiglitz – McBride Identification .....	21
3.2.1 Simulation Results .....	22
3.3 MATLAB™ Identification Tool .....	24
3.3.1 ARX Model .....	26
3.3.2 OE Model .....	26
3.3.3 BJ Model .....	27
3.3.4 ARMAX Model .....	28
3.4 Choice of Identification Model .....	28
3.4.1 Output Error versus Steiglitz-McBride .....	31
3.5 Implementation .....	31
3.6 Conclusion .....	32
<b>4 Implementation and testing of the SISO system .....</b>	<b>33</b>
4.1 Implementation .....	33
4.2 Testing of the SISO System .....	35

4.2.1	Results of the Test-implementation .....	35
<b>5</b>	<b>Total MIMO system including Cross-term compensation .....</b>	<b>37</b>
5.1	Introduction .....	37
5.2	Compensation Method.....	37
<b>6</b>	<b>Conclusions &amp; Recommendations.....</b>	<b>41</b>
6.1	Conclusions .....	41
6.2	Recommendations .....	42
<b>Appendix A : Simulation Results of the ARX Model.....</b>		<b>43</b>
<b>Appendix B : Simulation Results of the Output Error Model .....</b>		<b>44</b>
<b>Appendix C : Simulation Results of the Box Jenkins Model.....</b>		<b>45</b>
<b>Appendix D : Simulation Results of the ARMAX model.....</b>		<b>46</b>
<b>Bibliography.....</b>		<b>47</b>

# List of Abbreviations

ADC		Analogue to Digital Converter
ARMAX		Auto-Regressive Moving Average with eXogenous input model
ARX		Auto-Regressive with eXogenous input model
BJ		Box Jenkins model
DAC		Digital to Analogue Converter
DSP		Digital Signal Processor
FID		Free Induction Decay
MIMO		Multiple Input, Multiple Output
MSE		Mean Square Error
MRI		Magnetic Resonance Imaging
NMR		Nuclear Magnetic Resonance
OE		Output Error
RF		Radio Frequency
SIMO		Single Input, Multiple Output
SISO		Single Input, Single Output
St-McB		Steiglitz-McBride iteration
$B_0$	[T]	Static magnetic field
$g(t)$		Step response
$g'(t)$ and $g'[n]$		Compensated step response in continuous time and discrete time
$G(s)$		Laplace transform of the step response
$h(t)$		Impulse response
$H(s)$		Laplace transform of the impulse response
$u'(t)$ and $u'[n]$		Compensated input step in continuous time and discrete time
$u[n]$		Discrete time step input
$c_i$		i-th amplitude coefficient of the Eddy Current model
$\gamma$	$\left[ \frac{rad}{Ts} \right]$	Gyromagnetic ratio
$\varepsilon(t)$		Continuous time step input
$\tau_i$		i-th time constant of the Eddy Current model
$\omega_i$		i-th frequency component of the Eddy Current model, $\omega_i = \frac{1}{\tau_i}$
$\omega$	$\left[ \frac{rad}{s} \right]$	Larmor frequency
$\hat{y}$		Approximating function

# 1 Introduction

Magnetic Resonance Imaging (MRI) systems belong to the most advanced technical equipment in hospitals nowadays. These systems are used to make a tomographic scan of the human body. MRI fully depends on Nuclear Magnetic Resonance (NMR), this is the interaction of nuclei with an external magnetic field ( $B_0$ ). Nuclei with uneven atomic number possess a net angular momentum, or spin, which induces a magnetic moment [PHI]. When placed in a static magnetic field the magnetic moment will tend to assume discrete orientations, either with (parallel) or against (anti-parallel) the direction of the applied field. This alignment is not perfect, the spin-vector will experience a torque, which makes it rotate towards the axis of the applied field with a certain precise angular frequency. See Figure 1-1. This cone-shaped rotation is called the Larmor precession. The angular frequency associated with this phenomenon is called the Larmor frequency  $\omega$ .  $\omega$  is proportional with the applied magnetic field  $B_0$  [T]

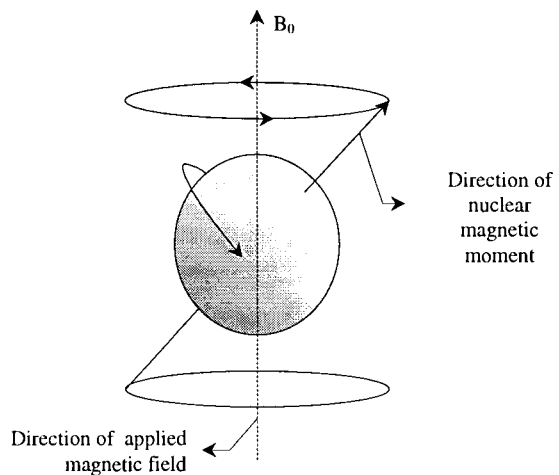


Figure 1-1: Precession of a spinning nucleus about the axis of an applied magnetic field

and the physical characteristics of the isotope: the gyromagnetic ratio  $\gamma \left[ \frac{\text{rad}}{\text{T s}} \right]$ :

$$\omega = \gamma \cdot B_0 \quad (1-1)$$

Due to the typically values of  $\gamma$  (order:  $10^7 \text{ radT}^{-1}\text{s}^{-1}$ ) and  $B_0$  (order:  $10^0 \text{ T}$ ) this Larmor frequency is in the Radio Frequency (RF) range (order:  $10^0 \text{ MHz}$ ).

Once the nuclei are aligned in the applied field  $B_0$ , they can be brought into resonance by a RF pulse with frequency  $\omega$ . During the relaxation process following the pulse the nuclei loose their energy by emitting RF signals, this is called the Free Induction Decay (FID). This FID-signal is detected by the RF coil, this can be the same coil that emits the RF signal, but in many cases this is a separate coil. It's strength depends on the concentration of nuclei under examination. This time-dependent FID signal yields a frequency spectrum from which the MR images can be calculated.

To introduce spatial dependency, there is a superposition of a magnetic field gradient on the static  $B_0$  field. The gradient is divided into three orthogonal directions x, y and z. Each having its own gradient coil, see Figure 1-2. Due to this magnetic field gradient, the nuclei the Larmor frequency varies proportional to the magnetic field gradient. In selecting a frequency for the RF-pulse to bring the nuclei into resonance, only the nuclei with that precise frequency will go into resonance. This way a certain

slice of the object under study (e.g. patient) can be selected. This can be in any orientation due to the three orthogonal directions of the gradient coils.

Most of the image techniques used nowadays, require short gradient switching times. This means the magnetic field gradient is changed rapidly. When a magnetic field changes it generates so called Eddy Currents in surrounding conducting materials. These Eddy Currents produce unwanted magnetic fields in the volume of interest and this causes artifacts in the image. One way of minimising the effects of Eddy Currents is by shielding the gradient coils. The disadvantages of this method is the reduced bore size due to the extra shield in the bore and it will not prevent Eddy Current fields originating from structures inside the gradient coil, such as Faraday screen, RF coil and conductive probe casing. To minimise the effects of Eddy Currents, a compensation method is employed. It is not possible to measure the gradient response when an object is being examined, this is why feed-forward control has to be used. The current driving the gradient is shaped in such way that the Eddy Current effects are eliminated. This is done by adding a certain overshoot to the input current waveform of the pulsed gradient. In this way, compensating for the linear Eddy Current fields. This overshoot is fully described by the system parameters and generated by the so-called pre-emphasis filters.

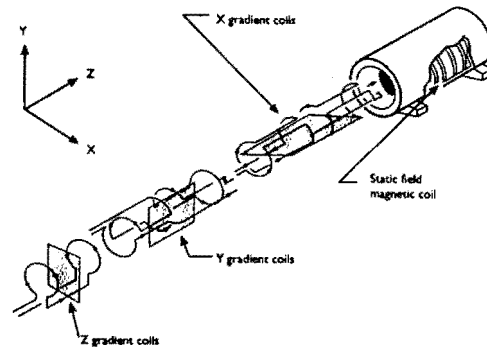


Figure 1-2: Typical coil arrangement in a MRI system.

The process referred to as: “Eddy Current compensation” is the minimising of the Eddy Current generated magnetic fields by adding an overshoot to the input waveform. Until now the tuning of these pre-emphasis filters is done manually. This is a time consuming, non-optimal method. An automated process can provide a more optimal and less time consuming solution of Eddy Current compensation. This is the reason this graduation project was started in corporation with Philips Medical Systems in Best, Netherlands.

Before designing an automated Eddy Current compensation, first the measurement of the gradient field and the manual Eddy Current compensation will be discussed. From this information the automated compensation is derived.

## 1.1 Measuring the Gradient Field Response

The gradient response can be measured using two different methods. One method uses pick-up coils to measure the gradient response. These pickup coils are mounted 15 cm. of the centre of the bore in the direction of the gradient under test, see Figure 1-3.

After placement of the pickup-coils, these coils are connected to a flux meter. The flux meter integrates the induced currents in the pickup coils, yielding a signal proportional to the time varying magnetic field at the position of the pickup coils. This



method has certain disadvantages. The coils react on a change in flux by generating a current and this current has a small amplitude. The analogue integrator is not optimal as it suffers from capacitor leakage. The following A/D converter works at the top of its range.

The other measurement method is the use of the FID-signal. A sphere filled with a

fluid is placed in the bore of the MRI scanner. The fluid consists of molecules with a magnetic moment. The disadvantage with this method is the fact that it requires a fully working MRI scanner, as one needs the RF coil to excite and to measure. Another disadvantage is the additional corrections that have to be made to get the actual gradient response. Advantages are that it has less measurement noise and is faster than the method with pickup coils.

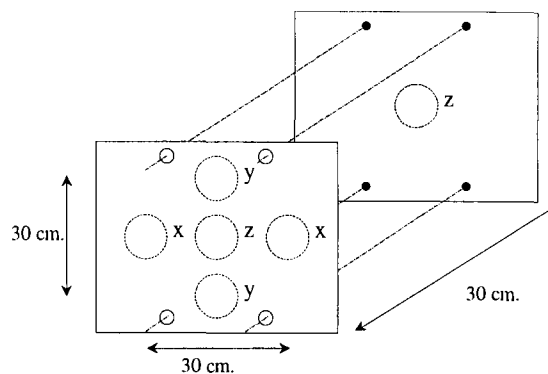


Figure 1-3: Positioning of the pickup coils.

## 1.2 Manual Eddy Current Compensation

In the present MRI systems the Eddy Current Compensation is done manually. A brief introduction into the modelling is necessary to understand the idea behind the manual compensation. The modelling will be fully discussed in Chapter 2.

### 1.2.1 Step Response Model in Short

For the modelling a step wave form is taken as the input signal for the gradient amplifier. This yields the following normalised step-response  $g(t)$ ,  $N$  represents the number of distinct Eddy Current decay terms present in the system and  $\varepsilon(t)$  is the input step function [MOR88]:

$$g(t) = \left( 1 - \sum_{i=1}^N c_i e^{-\frac{t}{\tau_i}} \right) \cdot \varepsilon(t) \quad (1-2)$$

This model is only valid under the assumptions that the system is linear and has single real poles. This model is used to explain the manual Eddy Current compensation. Ideally, the magnetic field generated by the step input would follow the step input, this is not the case due to the presence of Eddy Current in surrounded conducting material. In Equation (1-2) these Eddy Current are modelled as decaying exponential functions. Each of these functions has its own amplitude ( $c_i$ ) and time-constant ( $\tau_i$ ). The manual Eddy Current Compensation adds an overshoot that corresponds to these amplitudes and time-constant to the input step wave form to compensate the Eddy Current effect. See Figure 1-4.

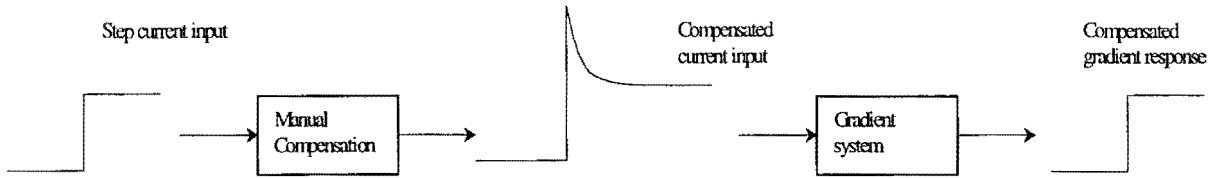


Figure 1-4: Basic idea of manual Eddy Current Compensation

### 1.2.2 Compensation Procedure

The manual compensation consists of several parallel high pass filters, with adjustable gain and time constant. Figure 1-5 gives a possible realisation of part of such a circuit. The time constant  $\tau_i$  is set by  $C_1$  and  $R_7$ , the relative amplitude  $c_i$  is set by  $R_3$ ,  $R_4$  and  $R_8$ . The total Eddy Current Compensation circuit has six of these similar sub-circuits, as denoted between the dashed lines .

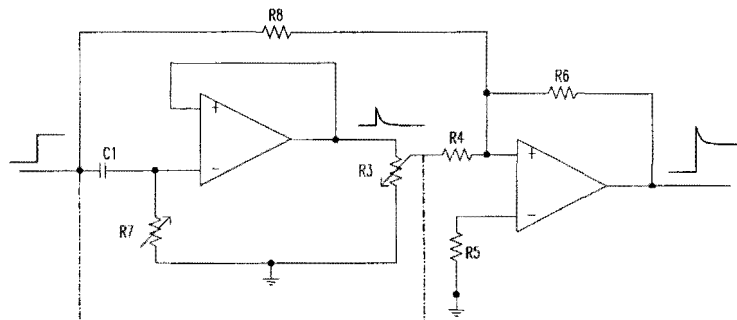


Figure 1-5: Pre-emphasis circuit for one exponential term, part of the total pre-emphasis filter.

Each section of this circuit has a dedicated time interval in which it works. This time interval is basically dictated by  $C_1$  . These time intervals are given in Table 1-1:

Table 1-1: Time intervals of the pre-emphasis circuits.

Filter	Operating range (ms)	
$c_6 / \tau_6$	200	3600
$c_5 / \tau_5$	40	640
$c_4 / \tau_4$	4	64
$c_3 / \tau_3$	0.4	6.4
$c_2 / \tau_2$	0.2	2.2
$c_1 / \tau_1$	0.03	0.33

The procedure of manual Eddy Current Compensation can be summarised in a few steps:

1. Place the pickup coils in the positions for the gradient under test (x, y or z) and connect them to the fluxmeter.
2. Execute the start-up checks: offset compensation of the flux meter and exact positioning of the pickup coils in the centre of the bore.

3. Switch on filter 6 of the Eddy Current Compensation. This is the filter with the largest time constant. Use the potentiometers to improve the flatness so that this is within the specification ( $< 0,1\%$ , see Table 1-2).
4. Repeat the previous step, but switch on filter 5 as well. Improve the flatness again. Continue this step until filter 3 is switched on.
5. Filter 3 operates in the range where the specification changes (see Table 1-1 and Table 1-2). With this in mind, improve the flatness using the potentiometers.
6. Switch on filter 2 and check the flatness again.
7. Finally switch on filter 1 and do a final check

The input step wave form is repeated every ten seconds with a duration of five seconds. This gives the Eddy Currents induced by the down ramp the time to completely die out. The above procedure has to be done for all of the gradient coils. One can imagine the total process, of manually compensating the Eddy Currents, is time consuming. Furthermore, this method is subjective and therefore different every time someone applies this manual Eddy Current Compensation.

Table 1-2: Specifications for the manual compensation of the present MRI system.

	PT1000A	Specification
$T_{avg}$ ( $\frac{3}{4}$ point)	0.45 ms	$71.0\% \pm 2.0\%$
$T_{avg}$	0.90 → 3.60 ms	$< 0.15\%$ flatness <sup>a</sup>
$T_{avg}$	3.60 → 990 ms	$< 0.10\%$ flatness <sup>a</sup>

Figure 1-6 gives a sketch of these specifications. The mean is set to be 100% and therefore this is valid. Both bands can shift in relation to each other. This means that an fluctuation of 0,2% in time interval 0,9 – 3,6 [ms] can still be within specifications, under the restriction that  $[\max.-\min.] < 0,15\%$  in this interval.

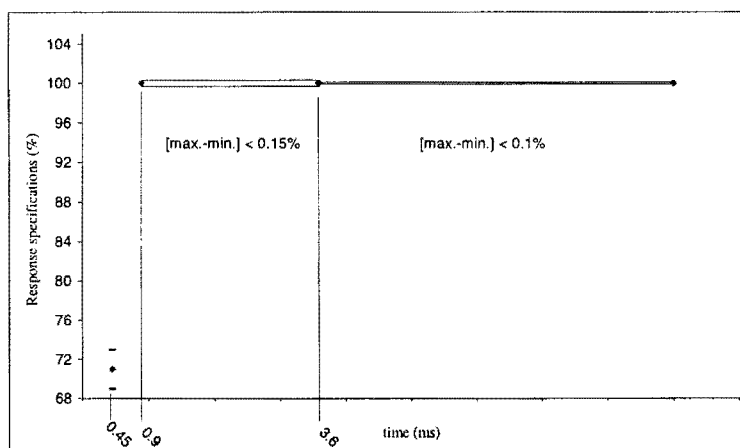


Figure 1-6: Schematic view of the flatness definition and its tolerance.

<sup>a</sup> flatness is defined as:

$$\left[ \frac{(\max. \text{ value}) - (\min. \text{ value})}{\left( \frac{(\max. \text{ value}) + (\min. \text{ value})}{2} \right)} \right]$$

## 1.3 Automated Eddy Current Compensation

The automation of the Eddy Current Compensation can, in first place, be seen as an automated parameter estimation. Which means the fitting of the uncompensated step-response will give the  $c_i$  and  $\omega_i$  of the Eddy Current transfer function and by using these, the pre-emphasis filter can be calculated. The method for fitting will be discussed in chapter 2. At this stage of the project, implementation can be anything between total software, DSP and total hardware (digital potentiometers) solutions. The identification of the system described above is what will be called the Compact System Identification.

Another way of identifying the system is to use a sampled step input and its sampled step-response in order to extract the discrete version of the impulse-response. By doing this the Eddy Current transfer function is obtained in the Z-domain. The pre-emphasis filter will therefore be a discrete filter. This method of identification will be referred to as being the Black-Box System Identification and will be discussed in chapter 3.

After analysing the different identification methods, a choice of identification method will be made. After implementation the system will be tested. Chapter 4 handles with all of this.

In chapter 5 the so-called cross-term and  $B_0$  shift will be discussed. That is, the compensation of these induced fields. Cross-terms are Eddy Current induced gradient fields in directions other than the applied gradient.  $B_0$  shift is a result of asymmetries in positioning to the gradient set. This gives a time-dependent change in the static magnetic field. This can also be compensated with the help of pre-emphasis filters [VAA90], [FRY97]. These pre-emphasis filters will have slightly different characteristics.

After this, this thesis concludes with the Conclusions & Recommendations in chapter 6, appendices and the List of Abbreviations.

## 2 Compact System Identification

### 2.1 Introduction

This identification method is based on the estimation of the parameters which characterise the Eddy Current behaviour. First a model will be set up to trace the parameters of the system. After that, a MATLAB™ simulation will be used to clarify the compensation based on the model. This will all be in a single input single output (SISO) fashion. Cross terms will be discussed later in Chapter 5.

### 2.2 Model for System Identification

As promised in paragraph 1.2.1, the Eddy Current model will be fully explained. The model used is based on electric circuits and often used in literature concerning Eddy Currents in MRI systems [JEH90], [VAA90]. Please note the model restrictions given in paragraph 2.2.2.

#### 2.2.1 Modelling with Electric Circuits

The multi-exponential decay of Eddy Currents can be modelled by  $L$ - $R$  series circuits, inductively coupled to the gradient coil  $L$ . See Figure 2-1.

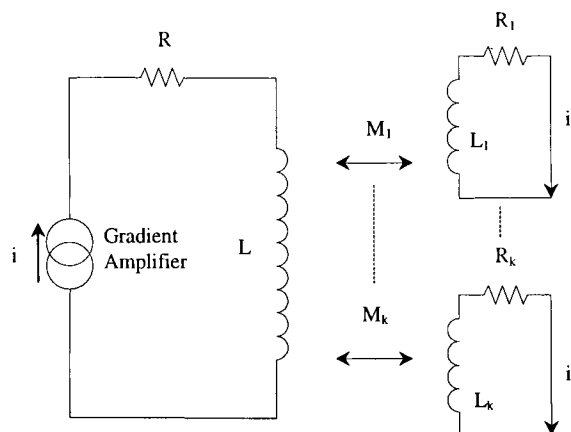


Figure 2-1: Eddy Currents are induced in loops, mutually coupled to the coil  $L$ .

The gradient amplifier forces a current  $i(t)$  through the gradient coil with resistance  $R$  and self-inductance  $L$ . The  $(L-R)_{1..k}$  circuits represent the electrical conducting structures of the MRI system in which the Eddy Current are induced. The total generated flux in the system is the superposition of the flux  $\varphi(t)$ , generated by the forced current in the gradient coil and induced Eddy Currents [JEH90]:

$$\varphi(t) = ai(t) + \sum_{k=1}^N a_k i_k(t) \quad (2-1)$$

with  $ai(t)$  is the gradient generated by the current in the gradient coil,  $a_k i_k(t)$  is the gradient generated by that Eddy Current and  $N$  is the number of coupled Eddy Current loops. Each Eddy Current  $i_{1..k}$  depends on the current  $i$  in the gradient coil according to:

$$L_k \frac{di_k(t)}{dt} + R_k i_k(t) + M_k \frac{di(t)}{dt} = 0 \quad (2-2)$$

By Laplace transform this yields:

$$sL_k I_k(s) + R_k I_k(s) + sM_k I(s) = 0 \Rightarrow$$

$$I_k(s) = -\frac{M_k}{L_k} \frac{s}{s + \frac{R_k}{L_k}} I(s) \quad (2-3)$$

Substituting this in the Laplace transform of equation (2-1) gives:

$$\Phi(s) = a \left( 1 - \sum_{k=1}^N c_k \frac{s}{s + \omega_k} \right) I(s) \quad (2-4)$$

where  $c_k = \frac{a_k M_k}{a L_k}$  and  $\omega_k = \frac{R_k}{L_k}$ .

Since the initial values of  $i(t)$  and  $i_k(t)$  are zero the following demand has to be met:

$$\sum_{k=1}^N c_k = 1 \quad (2-5)$$

Forcing a step current wave form into the gradient coil. Equation (2-4) becomes

$$\Phi(s) = a \left( 1 - \sum_{k=1}^N c_k \frac{s}{s + \omega_k} \right) \frac{1}{s} = a \left( \frac{1}{s} - \sum_{k=1}^N \frac{c_k}{s + \omega_k} \right) \quad (2-6)$$

This transforms back into:

$$\varphi(t) = a \left( 1 - \sum_{k=1}^N c_k e^{-\omega_k t} \right) \quad (2-7)$$

The Eddy-Current-generated contribution to  $\varphi(t)$  are modelled as a sum of exponential decaying gradients. The constant  $a$  is the steady state value of the gradient after all the Eddy Currents have decayed, for convenience the steady state value will be

normalised to  $a = 1$ . The same form was used in paragraph 1.2.1. Since  $\varphi(t)$  is in fact the step response of the system, the impulse response (yielding the transfer function) can be easily found:

$$h(t) = \frac{\partial \varphi(t)}{\partial t}$$

$$H_{E.C.}(s) = s \cdot \Phi(s) = s \cdot \left( \frac{1}{s} - \sum_{i=1}^N \frac{c_i}{s + \omega_i} \right) = \left( 1 - \sum_{i=1}^N \frac{s \cdot c_i}{s + \omega_i} \right) \quad (2-8)$$

The amplitudes,  $c_k$ , and time constants,  $\frac{1}{\omega_k}$  can be determined by multi-exponential fit of the gradient. In following paragraphs two methods for extracting these system parameters will be discussed. But first a word on the model and fitting of the step response.

### 2.2.2 Model Restrictions

In the above model the assumption is made, that the Eddy Currents are not mutually coupled. In fact (see Figure 2-1)  $L_l$  and  $L_k$  are indeed mutually coupled, but this does not affect the model in the end [JEH90], [VAA90].

The input is thought to be a step-function, where in fact the input signal is a ramp function. The gradient amplifier is physically not able to produce a step wave form current in the gradient coil. This means that there has to be a correction to go from step response in the model to the actual ramp response in the system. Another restriction is the assumption that the system is linear.

Furthermore, the model does not take into account the possibility of damped sine-functions in the Eddy Current fields. The gradient amplifier or the vibrating of the gradient coils can introduce these.

### 2.2.3 Fitting the Step Response

In single shot step response the total response is fit with exponential functions using the widely known non-linear least-squares fit method of Levenberg-Marquardt [PRE89]. This fit method has become the standard in non-linear least-squares routines and is very practical in use. It uses a  $\chi^2$ -merit function to deal with errors between data and fit, with  $\chi^2$  given as:

$$\chi^2(\alpha, \beta, \gamma, \dots) = \sum_{i=1}^n (f_i - \hat{f}_i)^2$$

where  $\hat{f}_i(x_i, y_i, z_i, \dots; \alpha, \beta, \gamma, \dots)$  is the approximating function, with  $\alpha, \beta, \gamma, \dots$  the unknown parameters.  $f_i(x_i, y_i, z_i, \dots)$  is the function to be approximated, i.e. the measured gradient response in this case.

Minimisation of the merit function proceeds iteratively, due to the non-linear character of the merit function,  $\chi^2$ . The Levenberg-Marquardt algorithm alternates elegantly between both the second derivative matrix (Hessian matrix) and the steepest decent method, to find the minimum of  $\chi^2$ . This way the minimum-approach is stable.

Because of this algorithm being fast and the standard of non-linear least squares routines, this algorithm was chosen. The unknown parameters estimated by the Levenberg-Marquardt algorithm are the Eddy Current parameters:  $c_k$  and  $\frac{1}{\omega_k}$ .

## 2.2.4 Single Shot Step Response

In the single shot step response method the gradient amplifier has a single step wave form input and the uncompensated gradient response is measured in the centre of the MRI system. The response can either be measured with pickup coils or the FID signal. The typical uncompensated step responses for the x-, y- and z-axes are given in Figure 2-2.

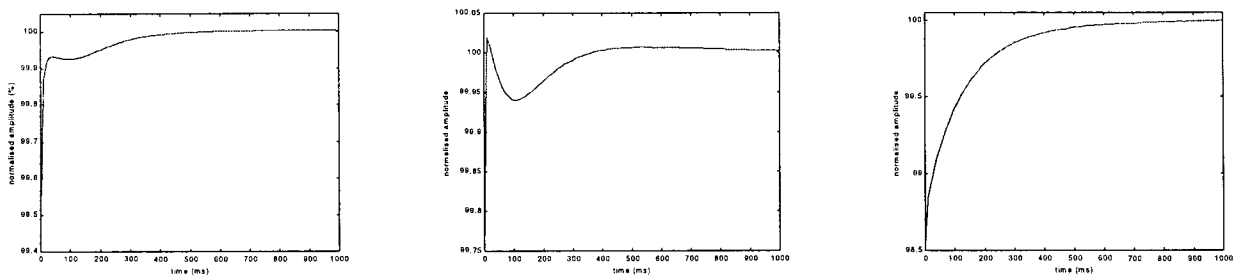


Figure 2-2: From left to right: normalised step responses of the x-, y- and z-axes.

All of these step responses are measured by using the FID signal. Due to the orientation of the different gradient coils, the step responses induce Eddy Currents with different parameters. This explains the variety of forms displayed in Figure 2-2. The reason that the uncompensated step response of the y-axis has an overshoot, can be explained as follows. A MRI system does not confine its magnetic field within the bore of the magnet, instead it spreads out in every direction. Therefore the present systems contain actively shielded gradient coils. This means the gradient coils is surrounded by an identical coil, only this surrounding coil is reversed in polarity, this way the Eddy Current fields induced by Eddy Current in conductive structures just outside the gradient coil are suppressed. In practice this suppression is never accomplished totally. When the outer coil (shielding coil) induces the majority of the Eddy Currents, this might happen due to physical movement of the outer coil, the uncompensated step response has an overshoot.

With these single shot step responses, the MATLAB™ simulation was carried out for Compact System Identification. The Eddy Current transfer function as given in equation (2-7), yields the following impulse response:



$$h(t) = \delta(t) - \frac{\partial}{\partial t} \left( \sum_{i=1}^N c_i e^{-\omega_i t} \varepsilon(t) \right) = \left( 1 - \sum_{i=1}^N c_i e^{-\omega_i t} \right) \delta(t) + \sum_{i=1}^N c_i \omega_i e^{-\omega_i t} \varepsilon(t) \quad (2-9)$$

Because of the nature of Eddy Currents and the decaying character of their generated gradient fields, this impulse response must be stable, which means  $h(t)$  has to converge to zero. This happens if and only if:  $\omega_i > 0$ , which will later be used as a demand for the automated parameter extraction in paragraph 2.3.1.

The Eddy Current transfer function will be inverted to get the optimal pre-emphasis filter. This gives the following expression for the pre-emphasis filter:

$$H_{pre}(s) = H_{E.C.}^{-1}(s) = \frac{1}{\left( 1 - \sum_{i=1}^N \frac{s \cdot c_i}{s + \omega_i} \right)} = 1 + \sum_{i=1}^N \frac{s \cdot \gamma_i}{s + \omega'_i} \quad (2-10)$$

One can analytically expand the summation of  $H_{pre}(s)$ ,  $\gamma_i$  and  $\omega'_i$  are functions of  $c_i$  and  $\omega_i$ , which can be extracted by a multi-exponential fitting procedure from the measured step response, see paragraph 2.2.3. This way the parameters of the pre-emphasis filter are known, but the dependency of  $\gamma_i$  and  $\omega'_i$  on  $c_i$  and  $\omega_i$  is quite complicated. A system representation comes in handy here.

Taking one step back, equation (2-7) can be interpreted as N parallel filters and a direct signal path. Figure 2-3 shows this system representation for the case N=6, all the leads are thought to be positive until mentioned otherwise:

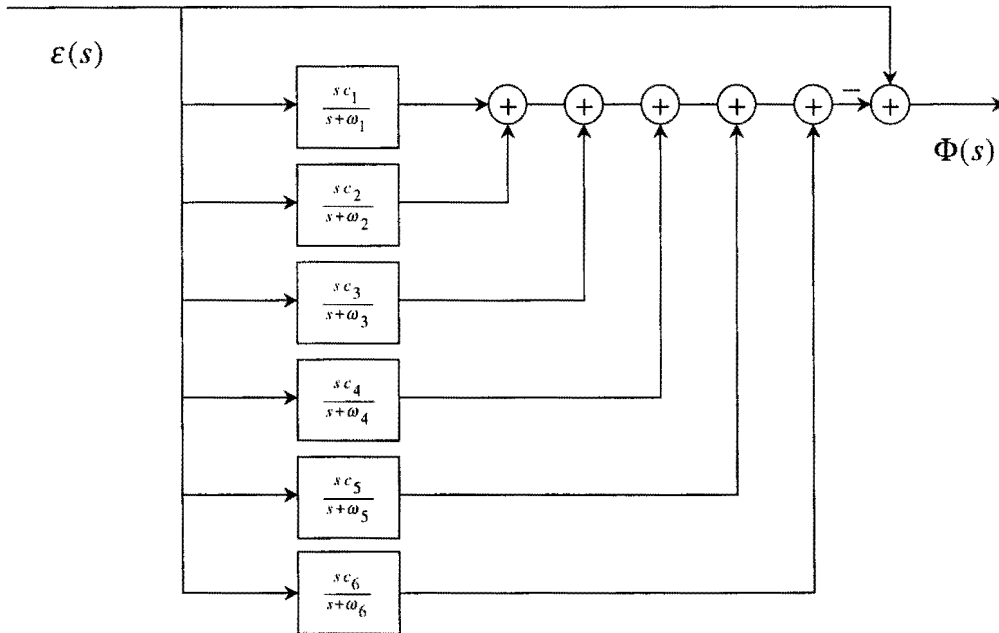


Figure 2-3: System representation of a 6<sup>th</sup> order Eddy Current transfer function.

As mentioned before the system parameters  $c_i$  and  $\omega_i$  can be extracted from the measured step response. By using the system representation, the Eddy Current transfer

function is much easier to interpret in a MATLAB environment. It gives the following notation for  $H_{E.C.}(s)$ :

$$H_{E.C.}(s) = \left( 1 - \sum_{i=1}^N \frac{s \cdot c_i}{s + \omega_i} \right) = \frac{num(s)}{den(s)} \quad (2-11)$$

This way the  $H_{pre}(s)$  is easily determined to be:

$$H_{pre}(s) = \frac{den(s)}{num(s)} \quad (2-12)$$

### 2.2.5 Multi Shot Step Response

As in the previous paragraph the parameters were all estimated in one go from the step response, in this multi shot method the parameters are estimated one by one. It becomes an iterative process, each time constant is estimated in the time interval where it is defined (see Table 1-1). The most common way is to first fit the step response for the largest time constant (e.g. time interval 200 - 3600 [ms]), then pre-filter with the found parameters.

Then generate another step input, with the compensation of the last found parameters active, and fit the response with a second, smaller time constant. The filter for the largest time constant is kept active, because the time intervals overlap. The second largest time constant operates for instance in the time interval 40 - 640 [ms], which can mean that the parameters found for the largest time interval have to be adjusted.

This is continued until the total number of time constants (N) is used to get the compensation within the specifications given (see Table 1-2). In literature this method is referred to as the backwards-correction procedure [MOR88]. Advantage of this method is the correction of the Eddy Currents generated by the compensation signal itself.

## 2.3 System Identification & Compensation

This section will discuss the actual system identification, using the single shot step response (see Figure 2-2). In the mathematical program MATLAB™, a procedure is written to fit a certain number (N, see Equation (2-2)) of exponential functions.

### 2.3.1 Algorithm

The algorithm is based on the MATLAB™ m-file `leastsq.m`. In this routine the Levenberg-Marquardt method is employed on the measured data, in this case the single shot step response. In order to do so it needs a number of time constants (N) as starting vector. This vector is used as a first approach for the fit and are initiated as follows:

$$\tau_n = \tau_1 4^{n-1} \Rightarrow \omega_n = \frac{1}{\tau_1 4^{n-1}} \quad (2-13)$$

By initiating the starting vector this way, the algorithm can also be used for systems developed in the future. If the starting vector consisted of the time constants now present in the system, this further usage would not be possible.

The number of time constants ( $n$ ) involved can be the following values: 3, 4, 5 or 6. The system has six major time constants, but sometimes the compensation can be achieved with a lower number of filters than six. A lower number of time constants than three does not give an acceptable fit, this is tested on the provided measurement data. Therefore fitting the step response for the number of time constants less than three will be left out of the discussion. The choice for the number of time constants is confirmed by the experience gained from the manual Eddy Current Compensation.

There are three condition for accepting the fit of the measured step response. All three of these conditions have to be met before the parameters, found in the fit procedure, can be used in the determination of the pre-emphasis filter:

1. One can easily see what happens if one of the estimated time constants is negative: the impulse response in equation (2-8) will become unstable, where the system itself should be stable.

$$\lim_{t \rightarrow \infty} \left( \left( 1 - \sum_{i=1}^N c_i e^{-\omega_i t} \right) \delta(t) + \sum_{i=1}^N c_i \omega_i e^{-\omega_i t} u(t) \right) = \lim_{t \rightarrow \infty} \left( \sum_{i=1}^N c_i \omega_i e^{-\omega_i t} u(t) \right) = 0 \quad (2-14)$$

Equation (2-14) holds only when:

$$\omega_i > 0 \quad \text{for } i = 1, \dots, N \quad (2-15)$$

Equation (2-15) is the first condition.

2. The amplitude of the separate exponential function has to stay within a reasonable bound, so that the gradient amplifier can handle it. This bound is set to  $\pm 1$  normalised to the amplitude of the step input. So the second criterion is:

$$|c_i| < 1 \quad \text{for } i = 1, \dots, N \quad (2-16)$$

The  $c_i$  is expressed in percentage of the normalised amplitude of the step input. Equation (2-16) is the second condition.

3. The value of the step response at the time of the step has to be larger than zero:

$$\varphi(0) \geq 0$$

substituted in equation (2-7), gives the third condition:

$$\left(1 - \sum_{i=1}^N c_i\right) \geq 0 \Rightarrow \sum_{i=1}^N c_i \leq 1 \tag{2-17}$$

When all of these conditions in (2-15), (2-16) and (2-17) are met, the parameters can be inserted in the model. It is understood that there will be a difference in the quality of the separate fits. To come to a choice of the set of parameters to use, a criterion is needed. This criterion has to determine which fit, of the measured step response, is the best choice. The parameters from this fit will be used in the actual pre-emphasis filter. As a criterion a general mean squared criterion can be used:

$$\sqrt{\sum (y - \hat{y})^2}$$

To accept the fit the criterion has to be in the order of  $10^{-3}$  (i.e. 0,1%), see Table 1-2. From system knowledge it is known that there are six time constants in the system, but it can happen that the order of the criterion is met for a lower number of time constants. This can be accepted as well, the result for the compensation is then used to decide whether the fit is acceptable.

### 2.3.2 Step to Ramp Response

Looking back at the model for the temporal Eddy Current field, in equation (2-7):

$$\varphi(t) = a \left(1 - \sum_{k=1}^N c_k e^{-\omega_k t}\right)$$

This model is based on the an arbitrary step input signal. As mentioned before this is not correct. The input signal is a ramp with a slope time in the order of 0,1 [ms]. So the model has to be corrected for the short-term effects of the Eddy Current influences. It will become clear that the long-term effects remain virtually the same. Because of the exponential character of the Eddy Current effects, this correction is an amplitude correction on the parameters found from the fit. This can be seen as follows:

Define the ramp function as:

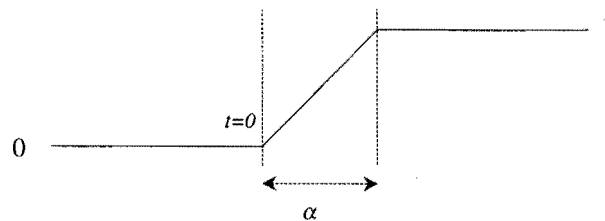


Figure 2-4: Ramp function.

This gives the following function:

$$r(t) = \frac{1}{\alpha} t \varepsilon(t) - \frac{1}{\alpha} t \varepsilon(t - \alpha) \quad (2-18)$$

where  $\alpha$  is the duration of the slope, see Figure 2-4. The Laplace transform of this ramp function yields:

$$R(s) = \frac{1}{\alpha s^2} (1 - e^{-\alpha s}) \quad (2-19)$$

The correction factor  $CORR(s)$  to go from the arbitrary step function to the ramp function, given in equation (2-18), can be calculated as follows:

$$R(s) = \frac{1}{s} CORR(s) \quad (2-20)$$

where  $\frac{1}{s}$  is the Laplace transform of the step function  $\varepsilon(t)$ . This gives:

$$CORR(s) = \frac{1}{\alpha s} (1 - e^{-\alpha s}) \quad (2-21)$$

Employing this correction on the model given in equation (2-7) means that every exponential in this model has to be multiplied with the correction factor. The Laplace variable  $s$  then becomes the pole  $-\omega_k$  [JEH90].

$$\frac{1}{\alpha \omega_k} (e^{\alpha \omega_k} - 1) \quad (2-22)$$

This means the parameter  $c_k$  found in the fitting procedure has to be corrected. The time constant remains the same. For time constants ( $\tau_k = \frac{1}{\omega_k}$ ) much bigger than the slope duration  $\alpha$  the amplitude correction is close to zero, whereas for time constants in the order of the slope duration the correction can be  $\frac{1}{1} (e^1 - 1) \approx 2$ .

### 2.3.3 System Parameters

With the algorithm present one can now identify the parameters of the system. As an example the case of a single shot step response on the y-axis will be worked out. This uncompensated response is as shown in Figure 2-5, the step to ramp correction is carried out so this is the step response.

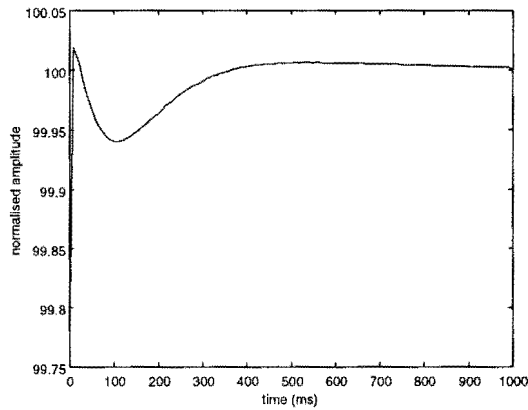


Figure 2-5: Step response of the y-axis.

First the number of time constants is set to three. When the conditions (2-14), (2-15) and (2-16) are met, the criterion value is calculated and stored. Then the number of time constants goes to four. And again all the criterion values are stored. This is also done for five and six time constants. After this the criterion values are compared with each other and the parameters from the best fit are chosen for the pre-emphasis filter. In this case the criterion did not improve significant when the order was raised from five to six, therefore the number of time constants was chosen five here.

In Figure 2-6 the result of this fit procedure is shown. The zoom-in part provides a better look around a critical area. The fit procedure aims to find the parameters  $c_i$  and  $\omega_i$  of the following model:

$$H_{E.C.}(s) = \sum_{i=1}^N \frac{s \cdot c_i}{s + \omega_i}$$

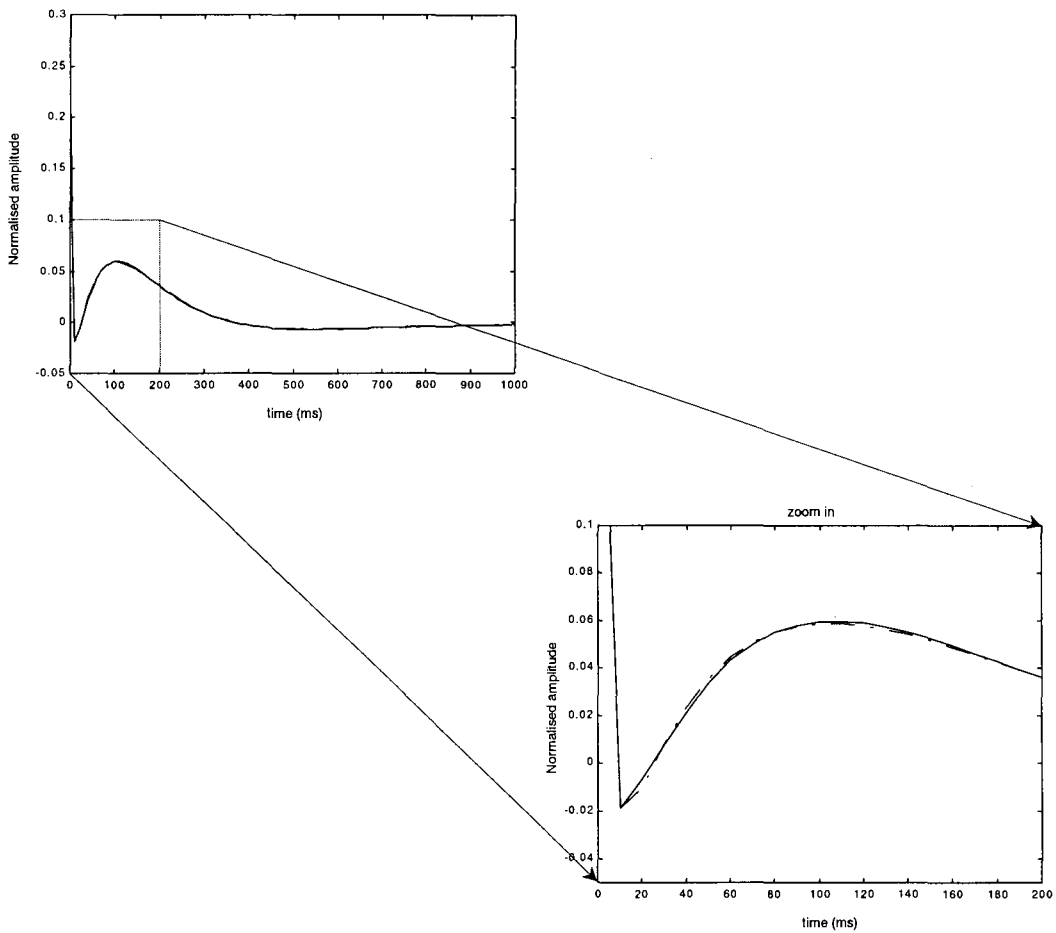


Figure 2-6: Y-axis single shot step response and its fit (dashed). The zoom in gives a better view of the critical area.

The error between the fit and the measured data is shown in :

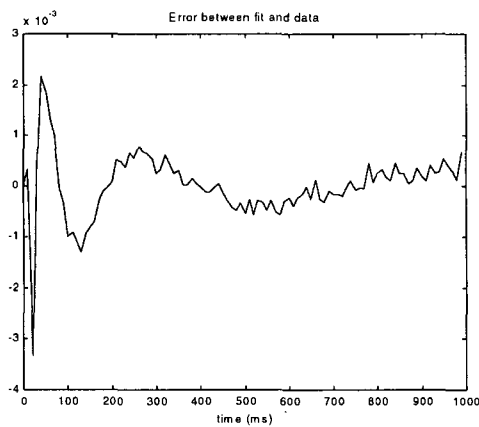


Figure 2-7: Fitting error for single shot step response of the Y-axis

Now that the system parameters are known, the Eddy Current transfer function is also known, see equation (2-8):

$$H_{E.C.}(s) = 1 - \sum_{i=1}^N \frac{s \cdot C_i}{s + \omega_i}$$

The compensation filter can now be calculated.

### 2.3.4 Compensation

Compensation can now be achieved by the pre-emphasis filter  $H_{pre}(s) = H_{E.C.}^{-1}(s)$ . A part of MATLAB™ called Simulink is used to create a simulation environment. Figure 2-8 depicts this structure:

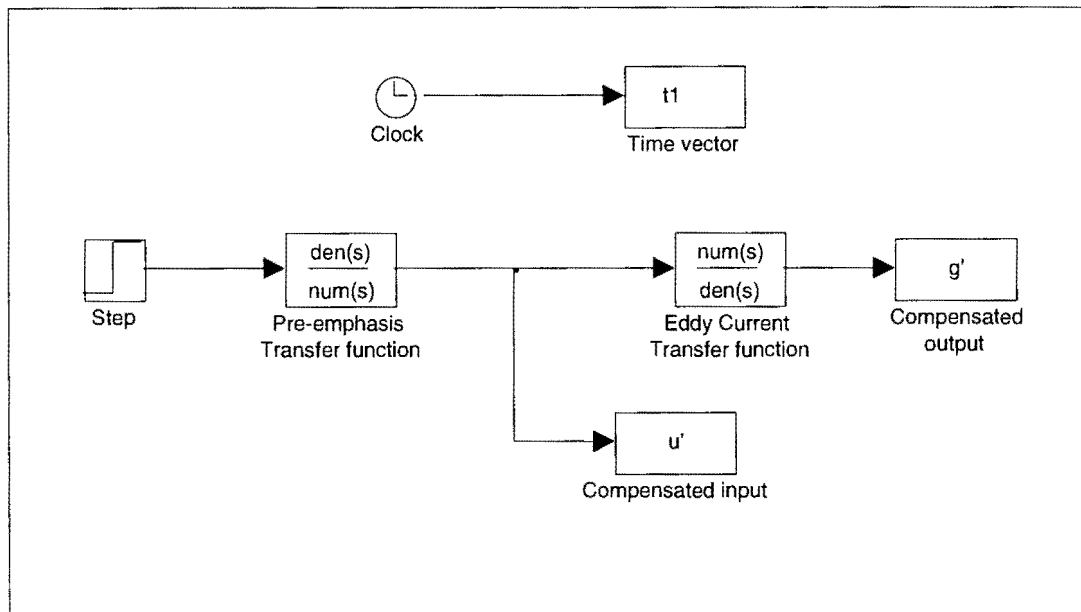


Figure 2-8: Simulink structure for simulation of compact system identification.

Substituting the found transfer function of the previously discussed example for the y-axis, in the Simulink structure, will give the following results (Figure 2-9):



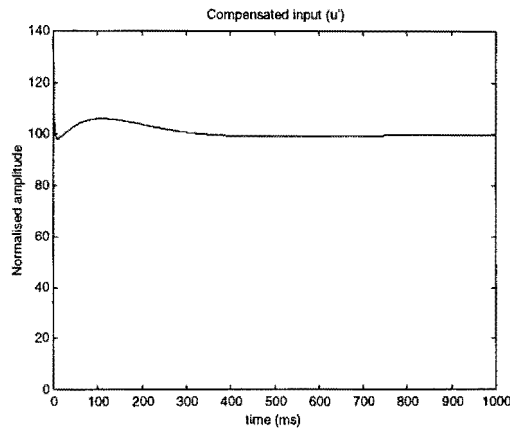


Figure 2-9: The compensated step input, as a result of the pre-emphasis filter.

This compensated input will have to bring the total Eddy Current field effect within the system requirements of 0.05 %. The compensated output of the Simulink structure, here denoted as  $g'$ , is as follows (Figure 2-10):

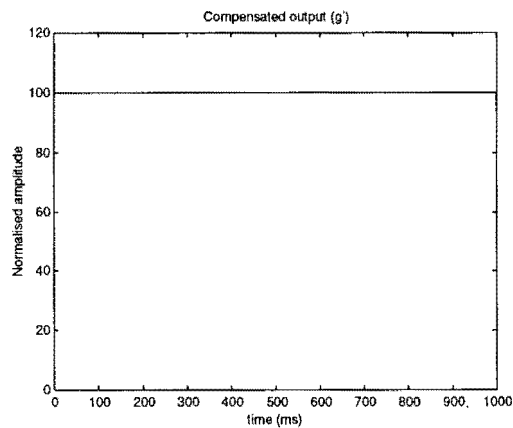


Figure 2-10: The step response, compensated for the Eddy Current field influences.

## 2.4 Conclusion

The identification and compensation procedure described in this chapter is comprehensive and provides the option of automation. This is why this method can be chosen to avoid the long and tedious manual adjustments as described in paragraph 1.2.2. This method can be implemented in present systems with only slight hardware adjustment.

However there are disadvantages to this method. As mentioned there are some model restrictions, see paragraph 2.2.2. The model needs a mathematical correction for the fact that the model is based on the use of a step input. Also effects like damped sine-functions are not accounted for, if there are complex poles these will not be identified.

Bottom line is that this method of identification and compensation could very well be successful. This method could be well worked out, implemented and work fine for the present systems, but there are too many disadvantages to not search for any further solutions. The method has to be reviewed thoroughly whenever a new system is developed, since this method requires a certain amount of a priori information.

## 3 Black-Box System Identification & Compensation

### 3.1 Introduction

Another way of identifying the system, is the use of black box identification. This method of identification uses the in- and output-signal to estimate the transfer-function and therefore a model of the system. This method of identification is widely used when there is no physical model of the process. There is a great variety of identification algorithms. The most important will be discussed, again making use of MATLAB™. All of these identification methods work in the discrete time domain, better known as the Z-domain.

At first the Steiglitz – McBride identification will be discussed in paragraph 3.2. The next paragraph is dealing with the general identification tool of MATLAB™ called `ident.m`. The ways of implementation of either of these black-box system identifications in the Eddy Current Compensation will be discussed in paragraph 3.5.

### 3.2 Steiglitz – McBride Identification

Steiglitz-McBride iteration [STE65] is an algorithm for finding an IIR filter. It has applications in both filter design and system-identification. This method returns the IIR filter coefficients in parameter vectors  $\mathbf{b}$  and  $\mathbf{a}$ . The filter coefficients are ordered in descending powers of  $z$ :

$$H_{E.C.}(z) = \frac{B(z)}{A(z)} = \frac{b_1 + b_2 z^{-1} + \dots + b_{m+1} z^{-m}}{a_1 + a_2 z^{-1} + \dots + a_{n+1} z^{-n}} \quad (3-1)$$

where  $m$  is the order of  $B(z)$  and  $n$  is the order of  $A(z)$ .

The Steiglitz – McBride iteration attempts to minimise the squared error between the estimated impulse response  $\hat{h}[n]$  of  $\frac{B(z)}{A(z)}$  and the impulse response  $h[n]$  given by  $g[n] = h[n] * u[n]$ , this latter is calculated out of the measured in- and output data :

$$\min_{a,b} \sum_{i=0}^{\infty} |h[n] - \hat{h}[n]|^2 \quad (3-2)$$

In order to show the usability of the method it will be demonstrated on the three step responses of the individual channels x, y and z. The setup is as follows:

1. Feed the step-input  $u[n]$  and the step-response  $g[n]$  into the Steiglitz-McBride algorithm.
2. Start with an order value for both  $A(z)$  and  $B(z)$  of: 3.
3. Make sure the  $H_{E.C.}(z)$  has no zeros outside the unit circle. These will become unstable poles in the  $H_{E.C.}^{-1}(z)$ .
4. Check  $H_{E.C.}(z)$  with a step input and compare this with the measured step response.
5. Use the same step input, but now as an input for  $H_{E.C.}^{-1}(z)$ , in order to get  $u'[n]$ , the compensated step input.
6. Now use the compensated step input  $u'[n]$  with the found  $H_{E.C.}(z)$  to check whether the compensated output is the same as the step-input.

Figure 3-1 gives a schematic view of the way the Eddy Current influences are compensated.

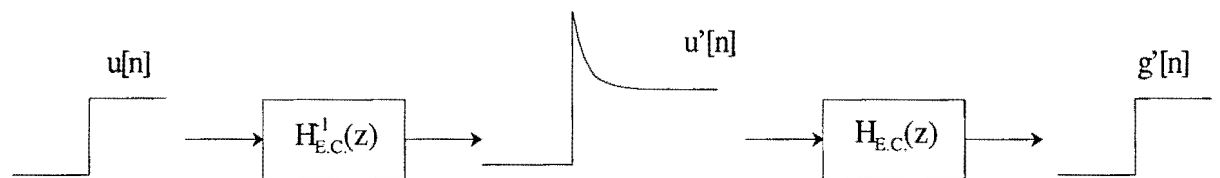


Figure 3-1: Schematic view of the compensation-process.

### 3.2.1 Simulation Results

The simulation results of the previous recipe for the three different axis are as follows:

- X-axis:

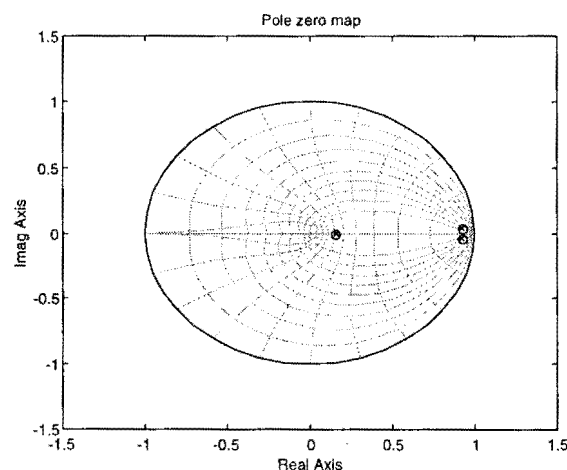


Figure 3-2: Step 3: check for zero's outside the unit circle.

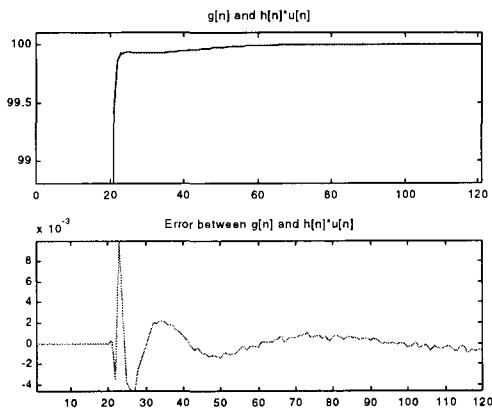


Figure 3-3: Step 4: check the identification.

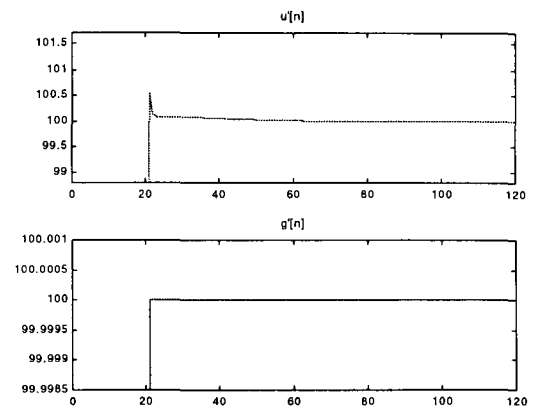


Figure 3-4: Step 5 & 6: check the compensation filter and output.

Y-axis:

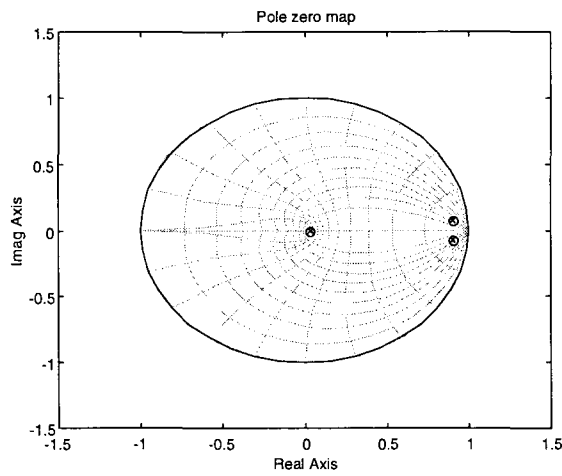


Figure 3-5: Step 3: check for zero's outside the unit circle.

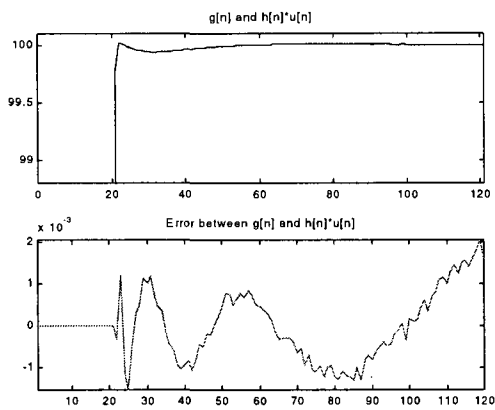


Figure 3-6: Step 4: check the identification.

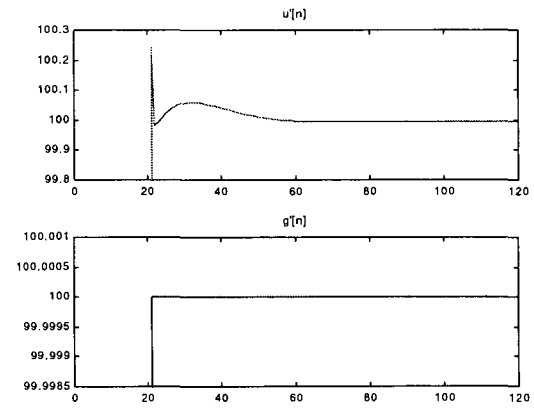


Figure 3-7: Step 5 & 6: check the compensation filter and output.

Z-axis:

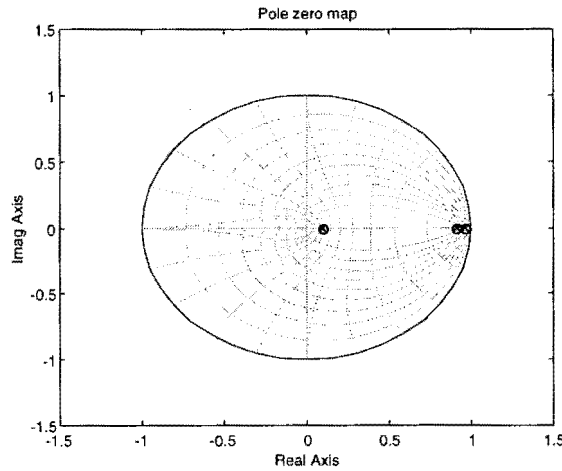


Figure 3-8: Step 3: check for zero's outside the unit circle.

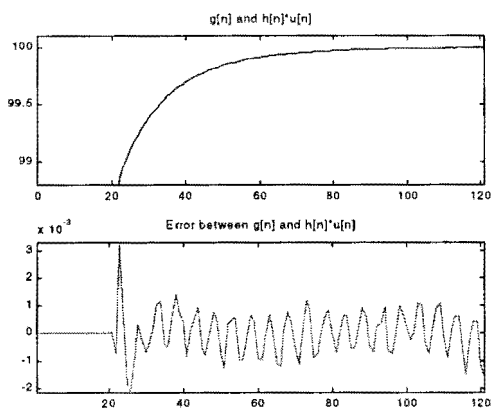


Figure 3-9: Step 4: check the identification.

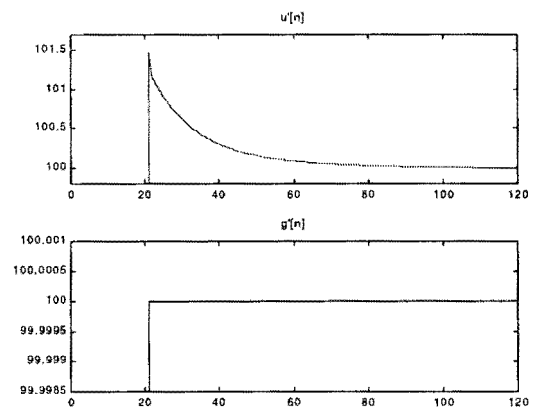


Figure 3-10: Step 5 & 6: check the compensation filter and output.

In step 4 the error is given as the difference between the two signals.

### 3.3 MATLAB™ Identification Tool

As mentioned before this identification tool: `ident.m`, is a general tool in the System Identification toolbox in MATLAB™. It employs the most common models for identification: ARX, ARMAX, OE and BJ [BOS94]. These are special cases of the general model:

$$y[n] = \frac{B(q)}{A(q) \cdot F(q)} u[n] + \frac{C(q)}{A(q) \cdot D(q)} e[n] \quad (3-3)$$

with:

$$A(q) = 1 + a_1q^{-1} + a_2q^{-2} + \dots + a_{n_a}q^{-n_a}$$

$$B(q) = b_1q^{-1} + b_2q^{-2} + \dots + b_{n_b}q^{-n_b}$$

$$C(q) = 1 + c_1q^{-1} + c_2q^{-2} + \dots + c_{n_c}q^{-n_c}$$

$$D(q) = 1 + d_1q^{-1} + d_2q^{-2} + \dots + d_{n_d}q^{-n_d}$$

$$E(q) = 1 + e_1q^{-1} + e_2q^{-2} + \dots + e_{n_e}q^{-n_e}$$

$$F(q) = 1 + f_1q^{-1} + f_2q^{-2} + \dots + f_{n_f}q^{-n_f}$$

Graphically this can be shown as in Figure 3-11:

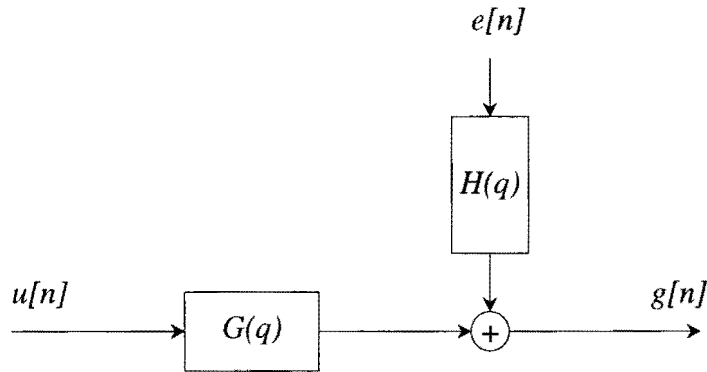


Figure 3-11: General model representation.

To keep the number of poles and zeros the same, the order for the polynomial  $B(q)$  is always one higher as that of the denominator, which can be either  $A(q)$  or  $F(q)$ , depending on the chosen identification model. The orders of the polynomials will be chosen different for each of the different axes based on a validation criterion. This validation criterion is the Mean Square Error (MSE), given by:

$$MSE = \sqrt{\frac{\sum (g[n] - \hat{g}[n])^2}{N}} \tag{3-4}$$

- where  $g[n]$  is the measured step response;
- $\hat{g}[n]$  is the simulated step response;
- $N$  is the number of data points.

The order of a model should not be too low, because then not all of the system dynamics can be described. On the other hand, the order should not be too high. Theoretically the increase of the model order beyond the true order should not improve the quality of the model. The MSE is a function of the model order, for each of the models this function is given. After this the different models can be compared with each other. For the in- and output signals of the simulation, see the Appendix A to Appendix D. The models ARX, OE, BJ and ARMAX will be worked out.

### 3.3.1 ARX Model

The Auto-Regressive with eXogenous input (ARX) model, is the derived from the general model by choosing  $C(q) = D(q) = F(q) = 1$ :

$$A(q)y[n] = B(q)u[n] + e[n] \tag{3-5}$$

The disturbance  $e[n]$  is modelled as AR-filtered white noise.  $u[n]$  is the exogenous input. This model is Auto-Regressive, because the output is a function of its past values:

$$A(q) = 1 + a_1q^{-1} + a_2q^{-2} + \dots + a_{n_a}q^{-n_a} \tag{3-6}$$

Figure 3-12 gives the relation between the MSE and the model order.

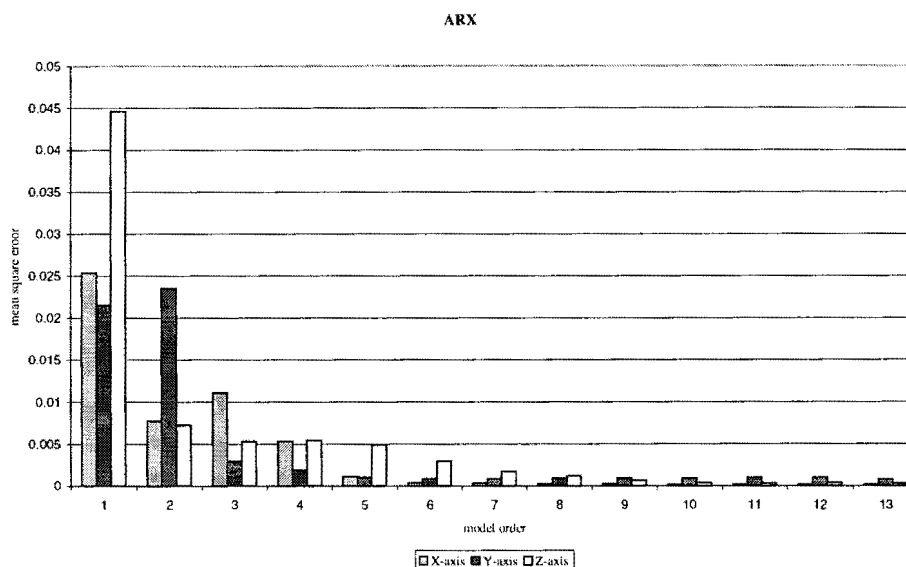


Figure 3-12: Mean square error for ARX models of different order.

### 3.3.2 OE Model

The Output Error (OE) model can be obtained from the general model, equation (3-3), by choosing  $A(q) = C(q) = D(q) = 1$ . The model then becomes:

$$y[n] = \frac{B(q)}{F(q)}u[n] + e[n] \tag{3-7}$$

The white noise disturbance is supposed to be additive to the output. Using this model the same procedure is followed to test the usability of this identification method. Figure 3-13 gives the relation between the MSE and the model order.



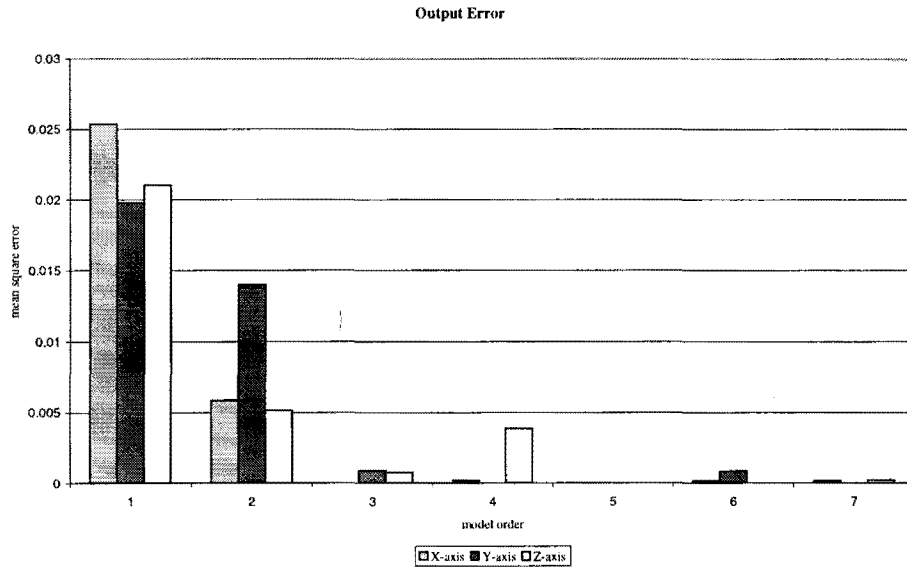


Figure 3-13: Mean square error for OE models of different order.

### 3.3.3 BJ Model

The Box Jenkins (BJ) model can be obtained from the general model, equation (3-3), by choosing  $A(q) = 1$ . The model then becomes:

$$y[n] = \frac{B(q)}{F(q)} u[n] + \frac{C(q)}{D(q)} e[n] \tag{3-8}$$

The plant model,  $G(q) = \frac{B(q)}{F(q)}$ , and the noise model,  $H(q) = \frac{C(q)}{D(q)}$ , have no parameters in common, therefore they are independently parameterised. Figure 3-14 gives the relation between the MSE and the model order.

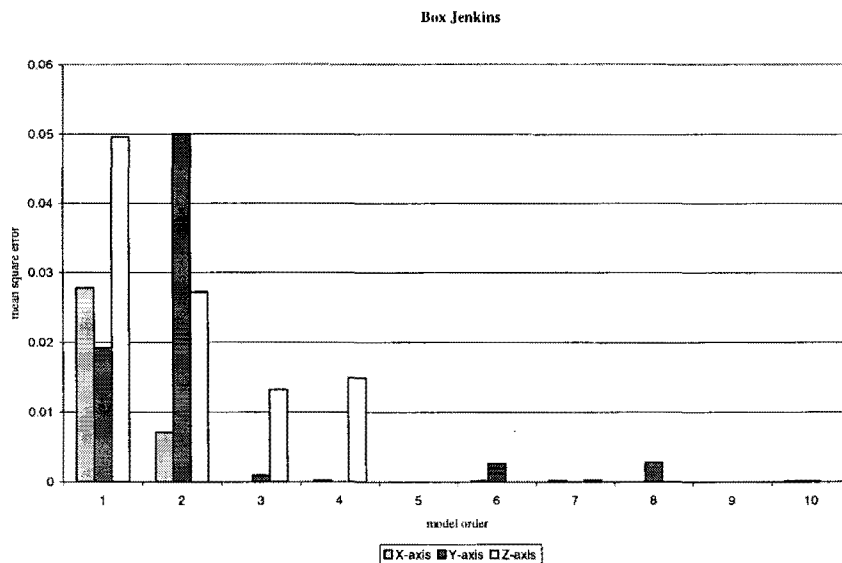


Figure 3-14: Mean square error for BJ models of different order.

### 3.3.4 ARMAX Model

The Auto-Regressive Moving Average with eXogenous input model, can be derived from the general model by choosing  $D(q) = F(q) = 1$ :

$$A(q)y[n] = B(q)u[n] + C(q)e[n] \Rightarrow$$

$$y[n] = \frac{B(q)}{A(q)}u[n] + \frac{C(q)}{A(q)}e[n] \tag{3-9}$$

Just as the ARX model, the ARMAX model is of the class of equation error models. The difference is that now the equation error is modelled as a MA process and the disturbance is now ARMA filtered white noise, additive to the output. Figure 3-15 gives the relation between the MSE and the model order.

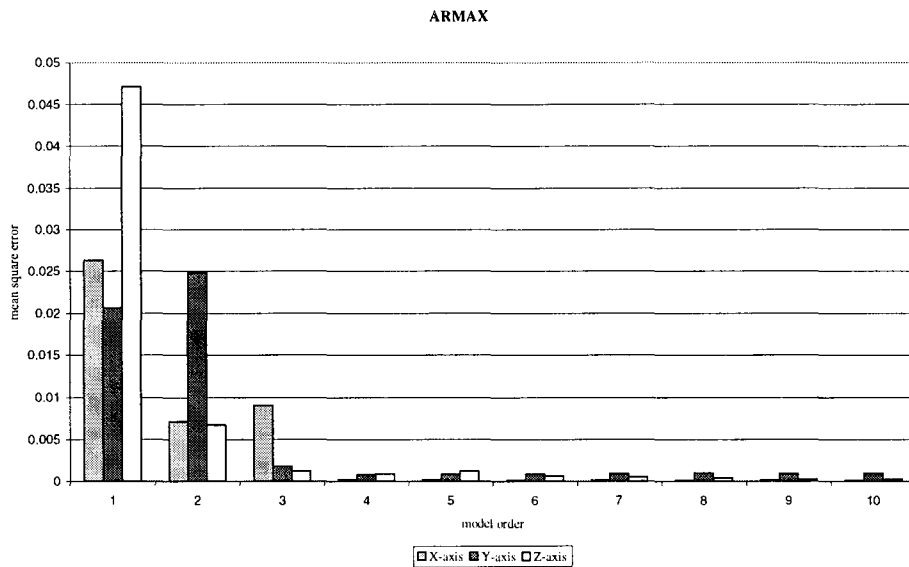


Figure 3-15: Mean square error for ARMAX models of different order.

### 3.3.5 St-McB model

The Steiglitz-McBride model, can be seen as a form of the general model by choosing  $A(q) = D(q) = 1$  and  $C(q) = 0$ :

$$y[n] = \frac{B(q)}{F(q)}u[n] \tag{3-10}$$

## 3.4 Choice of Identification Model

For the choice of the identification model the previous MSE as function of the model order can be used. For this purpose the MSE of all the models is collected for each of the separate axis.

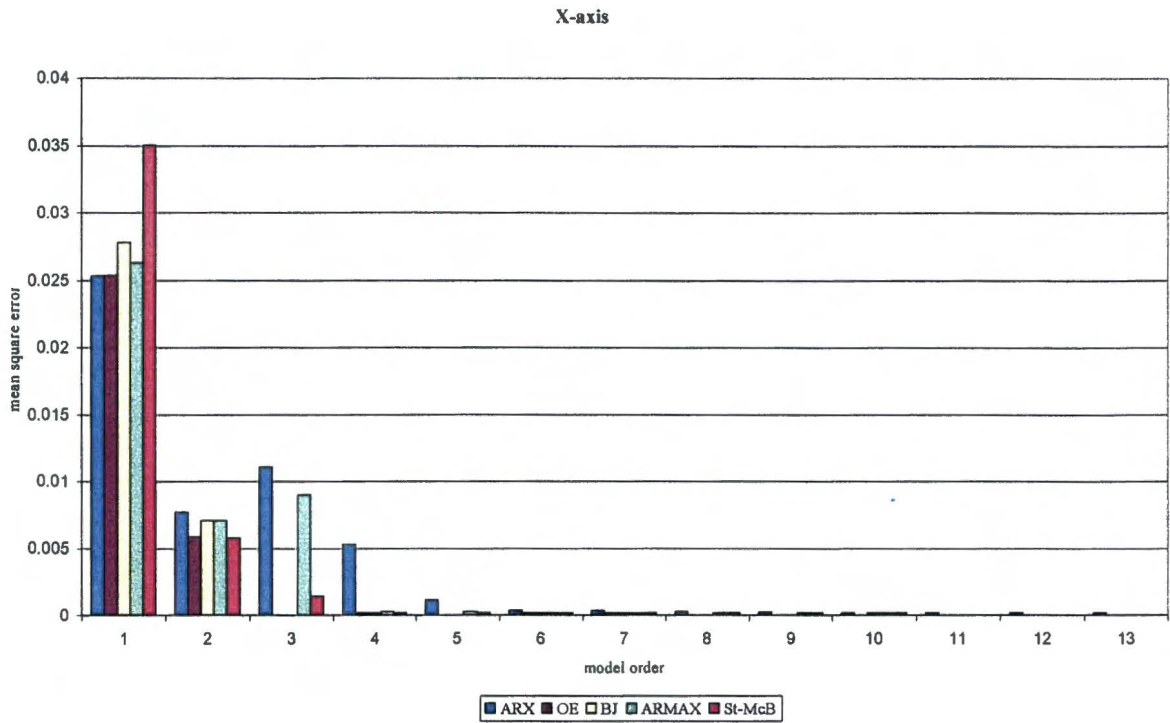


Figure 3-16: X-axis Mean Square Error for all the models, including Steiglitz-McBride, as function of the model order.

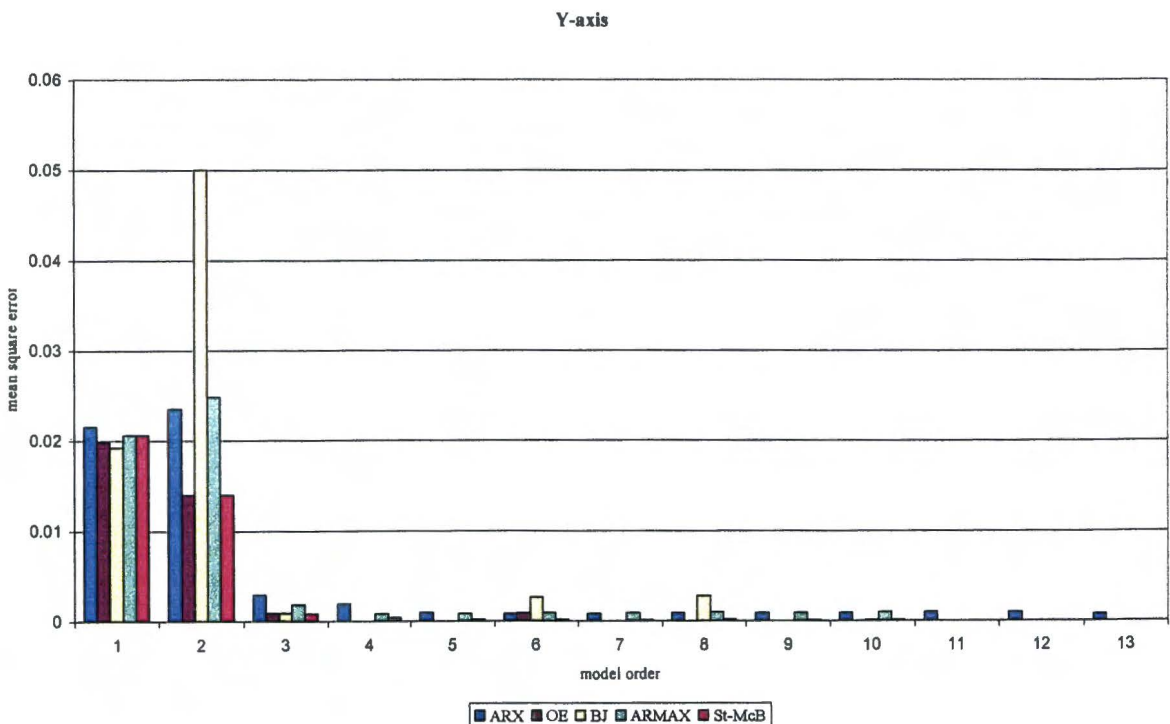


Figure 3-17: Y-axis Mean Square Error for all the models, including Steiglitz-McBride, as function of the model order.

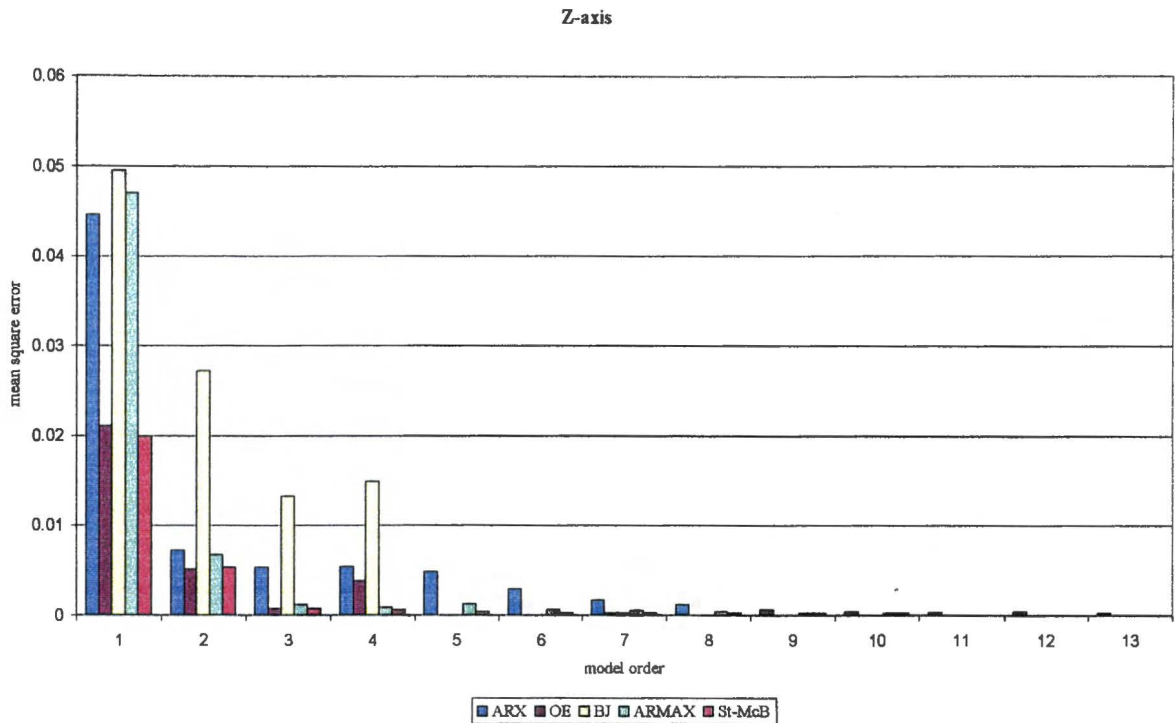


Figure 3-18: Z-axis Mean Square Error for all the models, including Steiglitz-McBride, as function of the model order.

What can be seen in the three graphs is that, for all the model, the MSE does not decrease significantly after a certain model order. The model order for which this virtual minimum MSE is reached is considered to be the model order to be used for the identification. Increasing the model order can result in getting the MSE toward zero. But in doing this not the process dynamics are modelled, but the noise contribution in the data set, yielding an incorrect model for another data set.

Another thing that can be seen from the above graphs is the difference between the different models. For instance the X-axis graph shows that the MSE reaches a virtual minimum for model order four when the OE model is used. In case the ARX model is used the MSE reaches this minimum for the model order of six. But the OE model does not give a good model estimation for the model order three, whereas the ARX model does give a reasonable estimate. This is probably caused by numerical instability of the OE model for certain orders. Looking at the Steiglitz-McBride model, the same value of the MSE is achieved for the same model order as OE. But more important it is numerical robust.

It can be concluded that for the X-axis there are basically three models which qualify for the system identification. All three of them have a model order of four. These models are:

- Output Error;

- Box Jenkins;
- Steiglitz-McBride.

For the Y-axis there are also three qualifying models with model order three:

- Output Error;
- Box Jenkins;
- Steiglitz-McBride.

In case of the Z-axis the models qualifying with model order three are:

- Output Error;
- Steiglitz-McBride.

So, based on the above observation one can make a choice of which model to be used for the system identification. The choice is between either the Output Error model or the Steiglitz-McBride model.

### 3.4.1 Output Error versus Steiglitz-McBride

The fact that Output Error and Steiglitz-McBride both remain is not surprising. The two models are very similar. However there exists a conceptual difference [ZHU93]. The output error aims to minimise the output-error-criterion or the MSE. The Steiglitz-McBride iteration is a specific iteration scheme, which is not a mathematical minimisation procedure. The Steiglitz-McBride iteration does not necessarily mean a decrease of the criterion after every iteration. No proof of convergence can be given, but under certain circumstances it can be proved that the estimates converge globally to the correct estimates [STE65], [STO81]. Out of the three references mentioned in this paragraph, is extracted that, from practical experience, the Steiglitz-McBride iteration does not significantly deviate from the Output Error model.

The Steiglitz-McBride iteration looks at the misfit of the model in frequency domain. The method is simple to understand and easy to use. Furthermore in the above simulations, the Output Error model occasionally has some numerical instability. For the Steiglitz-McBride iteration this was not the case.

Considering the features of Output Error, being theoretically more accurate than the Steiglitz-McBride iteration and the numerical stability of the Steiglitz-McBride iteration. Taking all of this into consideration, the choice has to be: the Steiglitz-McBride iteration.

## 3.5 Implementation

The best way to implement this black box system identification is to fully program it in software. All three of the discussed identification methods require some microprocessor for calculations in order to get to the best identification possible. A choice can be made between DSP or the terminal computer system. The latter offers a greater flexibility, whereas the DSP is smaller and in some cases faster.

For the test phase a system development DSP is used, which can be programmed via a normal personal computer. For the time being the pre-emphasis filter is calculated off line on the PC and then implemented on the DSP.

### 3.6 Conclusion

Based on the previous discussion the model used for black-box system identification is Steiglitz-McBride. There are a number of reasons for this choice. First the results of the simulations. In these simulations the MSE was chosen as the criterion. The minimisation of the MSE for the lowest order of the model is obviously a reason to choose that model. Here the Steiglitz-McBride iteration is performing significantly better as, say the ARX model, for a certain model order. The models equally performing: OE and BJ, experienced some numerical instability.

Further, the literature found on this Steiglitz-McBride model suggests this method performs equally well as the OE model. Third, the method is very easy to understand and use, because of the filter structure.

## 4 Implementation and testing of the SISO system

### 4.1 Implementation

For the test-phase, a DSP implementation is used. The system is tested for the single input, single output case (SISO). This means only one channel of the MRI system will be compensated (e.g. X-axis).

In the present MRI system the analogue voltage demand, which is fed into the analogue Eddy Current Compensation circuit and the gradient amplifier, can be brought out of the system. This creates a possibility to modify this voltage demand and create the compensated input. The system is identified off-line with the help of a PC. This PC loads the compensation filter into the DSP, the DSP filters the digitised voltage demand with the compensation filter. This results in the discrete time version of the compensated step input. This is converted into an analogue signal and then fed into the gradient amplifier. The manual Eddy Current Compensation is obviously switched off during these tests. A global schematic is given in Figure 4-1.

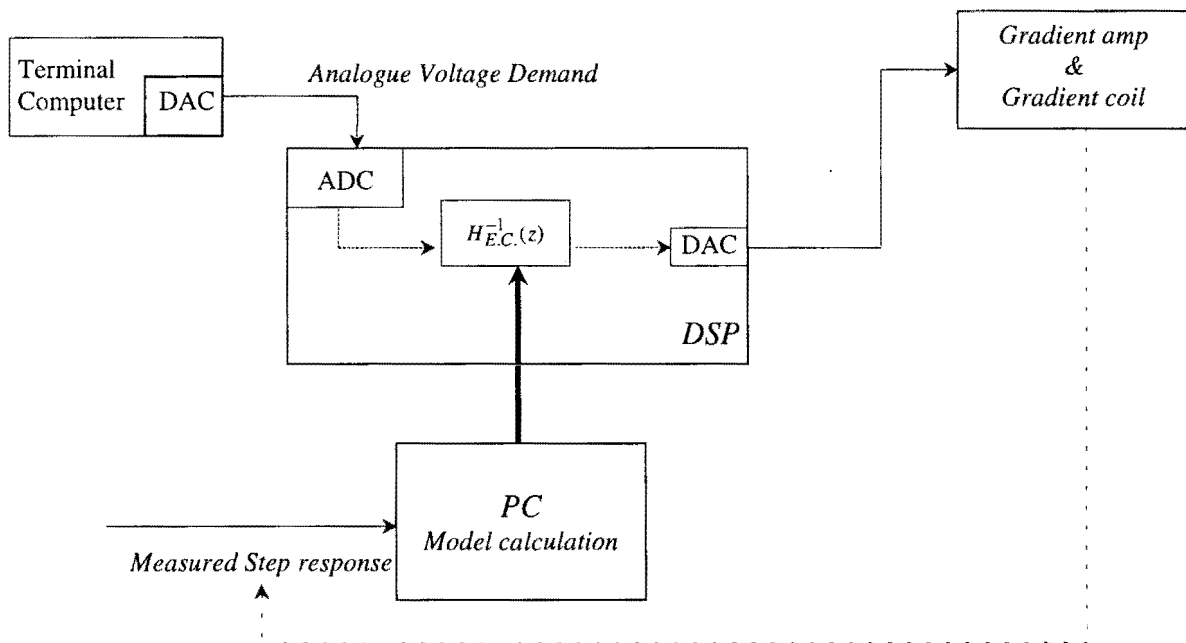


Figure 4-1: Schematic of the test implementation using a DSP

The analogue voltage demand, used as the input for the compensation as described above, is the result of D/A conversion from the digital voltage demand, generated by the workstation which controls the MRI system. That DAC is 16 bit and uses a sample frequency of 40 kHz. The reason for taking the analogue demand signal is that the

analogue demand signal is linked to the gradient amplifier externally. By modifying the connection it is possible to process the voltage demand. The digital voltage demand signal is not brought out of the system and therefore it is not possible to use the digital voltage demand, without major changes in hardware.

The analogue demand signal is a balanced, differential output, whereas the input of the ADC in the DSP is a single ended coax connector. This means the differential signal has to be converted to a single ended signal, using a differential amplifier. The other way around has to be done with the compensated input signal from the DAC in the DSP, the gradient amplifier requests a differential signal. For the differential to single end converter a standard instrumentation amplifier: INA 118. This amplifier uses the versatile three op-amp design as can be seen in Figure 4-2:

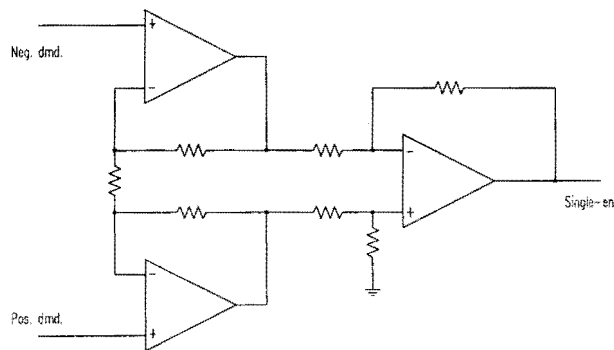


Figure 4-2: Schematic of the internal three op-amps design of the INA 118.

The circuit used to create the differential voltage demand from the single-end output from the DAC is shown in Figure 4-3. It uses two inverting op-amps to create the positive and negative demand.

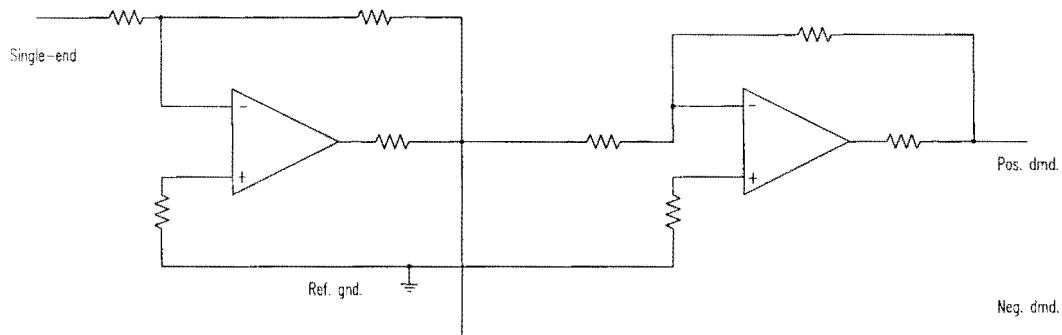


Figure 4-3: Schematic of the single-end to differential converter.

In both converter-circuits the overall gain is kept unity.

A future possibility is to make the compensation iterative. This means that the off-line system identification is implemented in the compensation loop. The consequence is that the initial compensation filter can be calculated using an arbitrary step input, but in the first iteration the digitised voltage demand is used as the input signal for the identification. The analogue voltage demand is typical a trapezium, duration of the trapezium is in the order of 1 [ms], the slopes are in the order of 0,1 [ms].



## 4.2 Testing of the SISO System

A number of sessions were needed in order to get a good result. A major problem was the sensitivity of the gradient amplifier. This gradient amplifier checks the voltage demand and switches in a so-called "signal error" when it detects something in the voltage demand what can not be made by the gradient amplifier. Because of the previously described converters from differential to single-end and vice versa, the voltage demand was disturbed by high frequency noise. The gradient amplifier detected that it could not create this current and therefore switched into "signal error".

Other disturbances were the glitches on the ground potential of the 220 [V] power supply. The DSP shared the same ground as the gradient amplifier. In the preparation phase of the MR measurement the amplifier switches into a standby mode. This caused a glitch on the ground potential, which could be seen in the compensated voltage demand. Resulting in a "signal error" from the amplifier. To overcome the above problems a first order low pass filter with a cut-off frequency of 66 [kHz] was implemented in the converter circuit. Furthermore a clean power supply was used to power the DSP. Occasionally the gradient amplifier switched into "signal error" during preparation phase, but this only occurred in a random fashion. This was no big problem for the test measurement, but should not be allowed in the final implementation.

Some software bugs caused further delay, but these could all be brought back to human interpretation.

After all these problems were overcome the automated Eddy Current compensation could be tested and the results were quite convincing. In the end the compensated system was within the system requirements of 0.05%. Partially due to the lack of time only the method described in chapter 2 was tested. This means the measured gradient field response of the uncompensated system was fit, the parameters were implemented in the derived model and from this the compensation filter was downloaded into the DSP.

From the experience gained by this compensation method the Black Box identification method can be fine-tuned. A further study of this problem will surely lead to an equally suiting result for the Eddy Current compensation.

### 4.2.1 Results of the Test-implementation

The result of the test with the DSP implementation is depicted in Figure 4-4. The solid line is the actual measured ramp response. This measurement is corrected for the measurement method and the ramp-to-step transform. The latter has been discussed in paragraph 2.3.2. In the measurement the actual signal measured is the integral over the interval  $t - t+4,28$  [ms]. The exponential is approximated as a straight line in this interval. The dotted line is the corrected signal

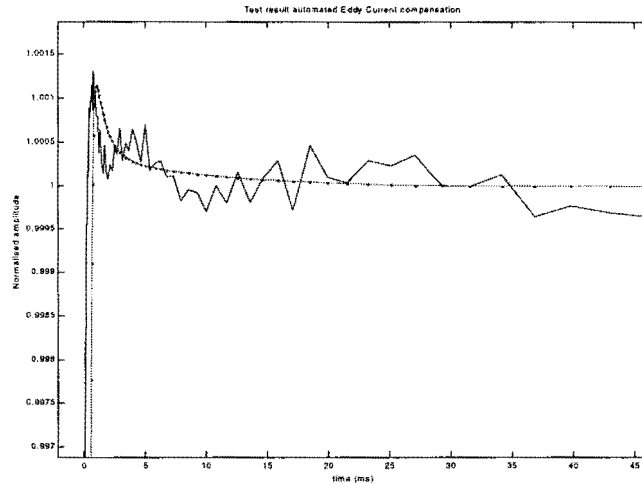


Figure 4-4: The measured step response of the compensated system.

It is clear that the dotted line is within the specifications given in Table 1-2. For Eddy Current effects in the time interval  $t \geq 3$  [ms] this step response is even within system specification, given to be 0,05%

The overshoot for  $0 \leq t \leq 3$  [ms] can be explained as follows. For short term Eddy Current effects with large amplitudes the error made in the measurement is about 3%. This means there can only be an improvement by a factor of 30. So, to get the Eddy Currents field response within the system requirements, for this time interval, the uncompensated deviation has to be smaller than 0.15%. This is absolutely not the case. Solution is to use this compensated step response and identify the Eddy Current compensation a second time, in other word make the process iterative. With just one iteration the above system can be brought within system specification.

In order to speed up the measurement, one could divide the time-interval in a long term part and a short term part. For the long term part no iteration is needed and the measurement only has a maximum systematic error of 0,01%. The short term part can be iteratively identified. The long term compensation does influence the short term behaviour, so the long term compensation should be kept active during the iteration. This approach can be further studied in order to speed up the measurement.

## 5 Total MIMO system including Cross-term compensation

### 5.1 Introduction

The implementation tested in the previous chapter describes a compensation of a single input, single output system. The Eddy Current field does not necessarily have the same orientation as the field it is originating from. If, for instance, the X-axis gradient coil is used, there will be Eddy Current fields in the Y- and Z- direction. These fields are called the cross-term Eddy Current fields. This chapter will propose the compensation needed, to minimise the effect of the cross-terms.

### 5.2 Compensation Method

In Figure 5-1 a schematic is given for the Cross-term Eddy Current compensation [VAA90].

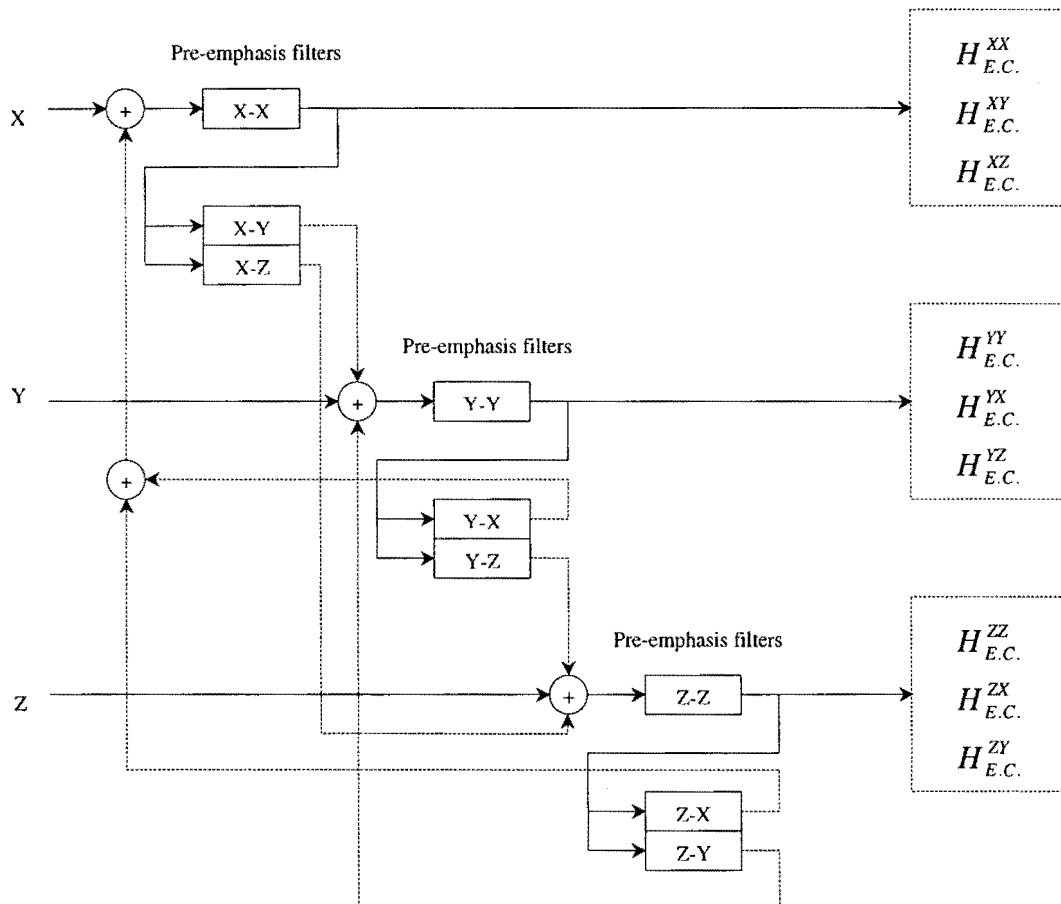


Figure 5-1: Schematic of the total pre-emphasis system including cross terms and the compensation of the  $B_0$ -shift.

To compensate the Eddy Current Cross-terms the following pre-emphasis filter have to be identified:

- XY;
- XZ;
- YX;
- YZ;
- ZX;
- ZY.

Since the procedure of identification and compensation is the same for all the Cross-terms, only the XY cross-terms will be worked out as an example.

The Eddy Current Cross-terms can be seen as (in s-domain):

$$B_{XY}(s) = I_X(s) \cdot XX(s) \cdot H_{E.C.}^{XY} \quad (5-1)$$

where  $B_{XY}(s)$  is the Eddy Current Cross-term field;

$I_X(s)$  is the input current;

$XX(s)$  is the pre-emphasis filter for the symmetrical Eddy Current field;

$H_{E.C.}^{XY}$  is the transfer function for the Eddy Current Cross-term.

From the schematic in Figure 5-1, the compensation field,  $B_{XY}^{corr}$ , is:

$$B_{XY}^{corr}(s) = I_X(s) \cdot XX(s) \cdot XY(s) \cdot YY(s) \cdot H_{E.C.}^{YY} \quad (5-2)$$

where  $B_{XY}^{corr}(s)$  is the compensating field;

$H_{E.C.}^{YY}$  is the transfer function for the symmetric Eddy Current field.

The Cross-terms will be compensated when:

$$B_{XY}^{corr}(s) = -B_{XY}(s) \quad (5-3)$$

This yields:

$$I_X(s) \cdot XX(s) \cdot XY(s) \cdot YY(s) \cdot H_{E.C.}^{YY} = -I_X(s) \cdot XX(s) \cdot H_{E.C.}^{XY} \quad (5-4)$$

Ideally the symmetric Eddy Current fields should be fully compensated, so:

$$YY(s) \cdot H_{E.C.}^{YY} = 1 \quad (5-5)$$

Using this assumption, equation (5-4) becomes:

$$I_X(s) \cdot XX(s) \cdot XY(s) = -I_X(s) \cdot XX(s) \cdot H_{E.C.}^{XY} \quad (5-6)$$

So the Cross-term compensation pre-emphasis filter,  $XY(s)$ , is:

$$XY(s) = -H_{E.C.}^{XY} \quad (5-7)$$

As mentioned before this procedure is mathematically the same for all of the Cross-terms, XY, XZ, YX, etc. But the above compensation method only holds for the case of SIMO, i.e. when only one input channel is used.

Now the problem is brought back to a similar problem as in the previous chapter. The uncompensated gradient field response has to be measured with the symmetric Eddy Current compensation switched off. This way the Cross-term transfer function can be identified. Either compact system identification (chapter 2) or black-box system identification (chapter 3) can be used.

There is however a problem on translating this to the MIMO system. Assume that every pre-emphasis filter has order six, this means the total MIMO system has an order of 54. That is when all the separate pre-emphasis filters are identified independently of each other. So the MIMO system in Figure 5-1 is not a minimum realisation of the system, which in turn means there are certain poles in the system, which are separately identified, but are in fact the same. Problem is to handle a criterion, which can make the decision whether these poles are identical or not.

As an example the pole-zero map is given from the filters XX, YY and ZZ. See Figure 5-2. These filters are identified for order three to preserve clarity of the plot, furthermore the z-grid is not displayed for the same clarity reason. As can be seen the real poles and zeros towards the origin are well separated. The other poles and zeros all have a real part around 0,9. The imaginary part is either zero or very small. This can suggest that these poles and zeros are in fact identical, but no certainty can be given. Solution of this problem could be a black-box MIMO identification.

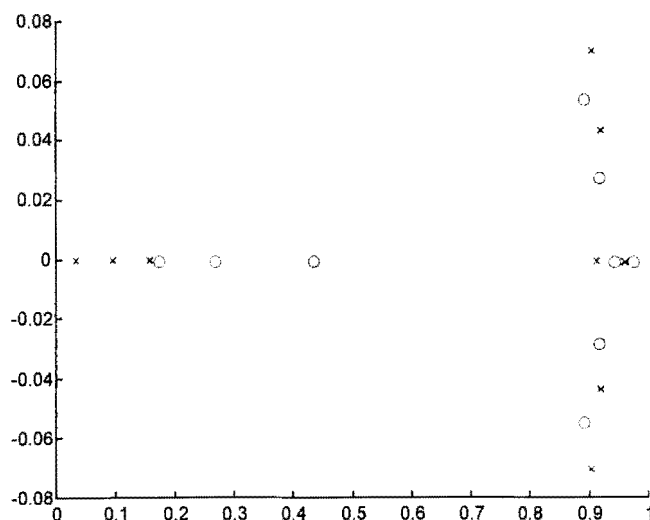


Figure 5-2: Pole-zero map in z-domain

Given this problem the above described method of SIMO, might very well work in the MRI system. All the individual pre-emphasis filters are stable and can be modelled as the sum of decaying exponential functions. Unfortunately no simulation has been done for the MIMO case, due to lack of time and not having an appropriate data-set. It is recommended to examine this method of MIMO identification .

## 6 Conclusions & Recommendations

### 6.1 Conclusions

The subject of this project was to study the possibility of designing an implementing a control system to automate the compensation of Eddy Current fields in an MRI system. Eddy Current fields distort images and spectra created by an MRI system. The Eddy Current fields are induced by pulsed magnetic gradient fields, these gradient fields are needed to create an image or spectrum. After literature study on this subject a general idea of the compensation method was formed. Basic idea is to identify the Eddy Current field behaviour. Then invert this behaviour and pre-emphasise the magnetic gradient pulses. By doing so the Eddy Current influences can be compensated. In present systems this compensation is done manually, which is a time consuming and tedious job.

The design of the pre-emphasis filter is divided in two parts. First, a model was created. This model expresses the transfer function of the current wave form in the gradient coil to the measured gradient field. Eddy Current can be modelled as a sum of exponential decaying terms. The amplitudes and time constants of these exponential terms can be identified by fitting the measured step response of the gradient field response. This continuous time method is called the compact system identification. Second, a black-box identification was studied. Here a priori knowledge of the system is not needed. The model is identified using only the in- and output wave forms. Standard black-box identification models were used, such as ARX, OE, Box Jenkins and Steiglitz-McBride iteration. This discrete time method is obviously called black-box system identification. Computer simulations were used to study both the results from compact system identification and black-box system identification. These simulations gave satisfying results.

The compact system identification has the disadvantage that it needs a priori system knowledge. Furthermore, the model derived has restrictions: only real poles can be identified. This way damped sine functions won't be identified, which are present in some configurations of MRI systems. This method has been implemented in a DSP and tested on a real MRI system. Resulting in an Eddy Current compensation within specification. This confirms the theory, based on simulation, that Eddy Current fields can be automatically compensated.

The black-box identification proved to be working correct as well in simulation. Unfortunately this is not tested on the real MRI system. This was due to lack of time and some software bugs while implementing it in the DSP. But since only the approach in getting the model differs conceptual and the model itself should not, there is a certainty that this method will also be able to automate the Eddy Current field compensation. The black-box has the advantage of not needing a priori system knowledge and can therefore be readily used in future MRI systems. Furthermore, when the compensation is studied as a MIMO system, the compact system identification does not give a minimum realisation and does not recognise to state

being the same, even if they are. But with the help of black-box identification it might very well be possible. Which will be recommended in the next paragraph.

## 6.2 Recommendations

Bottom line is that the Eddy Current field compensation can be automated, but it is recommended that some things are further investigated. First there is the testing of the black-box identification. This method has the slight edge above compact system identification, because of future development of the MRI systems, the absence of a priori system knowledge and the possibility of identifying damped sine functions.

Second, it is recommended to further study the MIMO system. It can be a good thing to individually identify all the pre-emphasis filter of the total MIMO system and test this implementation of the non-minimum realisation. A strong feeling exists that it still might work, because all the pre-emphasis filters stable. And when compact system identification is used all the poles of these filters are real as well.

A third recommendations is to see whether iteration for separate time intervals can speed up the measurement. It might be possible to compensate the short term Eddy Currents ( $\leq 100$  [ms]) virtually in real-time. Further study therefore is recommended.

Overall conclusion is that the start into automated Eddy Current compensation is made and the tests show a very satisfying result. The present manual Eddy Current compensation can most certainly be automated. To include the cross-term Eddy Current fields is looking to be a bit harder to identify, but further study will surely clarify this problem.



# Appendix A : Simulation Results of the ARX Model

- X-axis:

The order of  $A(q)$  is six, the order of  $B(q)$  is seven.

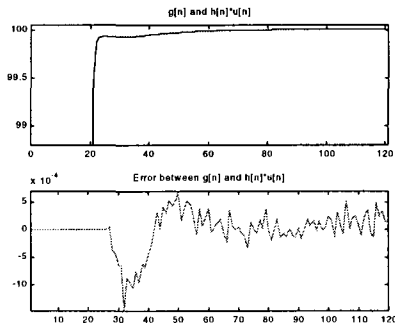


Figure 6-1: Check the identification.

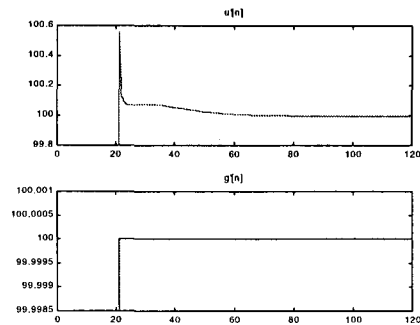
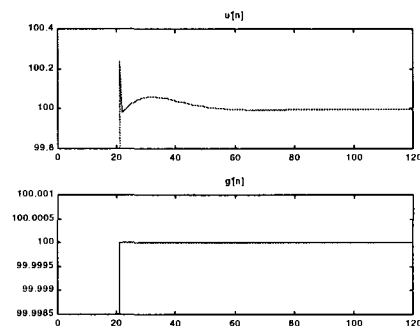
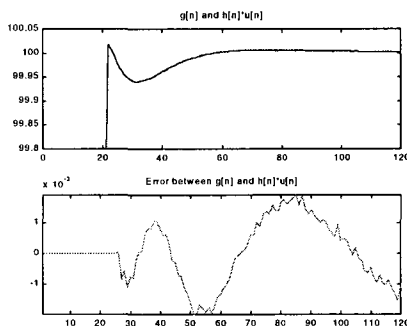


Figure 6-2: Check the compensation filter and output.

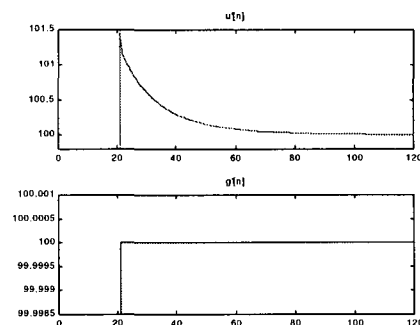
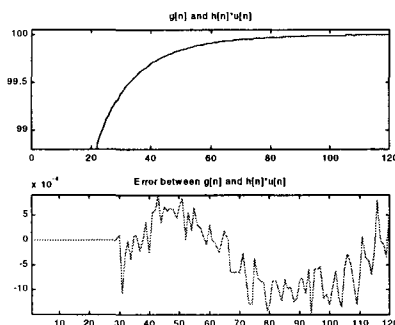
- Y-axis:

The order of  $A(q)$  is five, the order of  $B(q)$  is six.



- Z-axis:

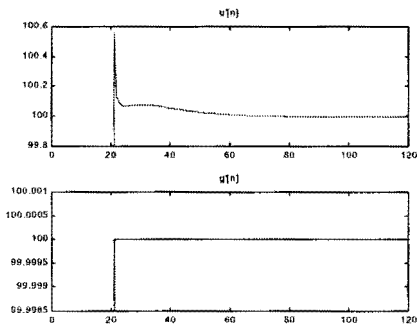
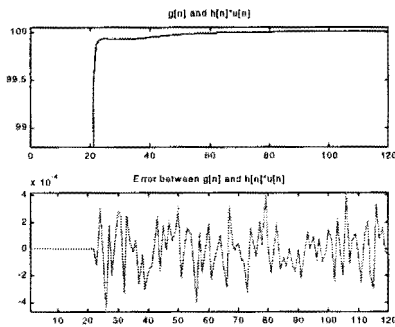
The order of  $A(q)$  is nine, the order of  $B(q)$  is ten.



# Appendix B : Simulation Results of the Output Error Model

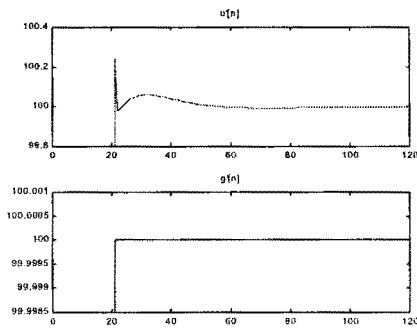
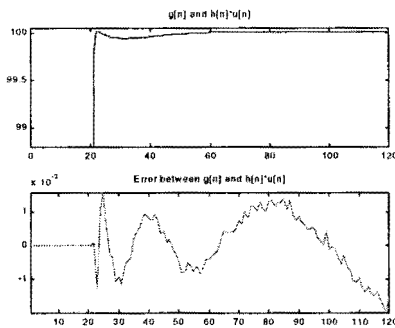
- X-axis:

The order of  $B(q)$  is five, the order of  $F(q)$  is four.



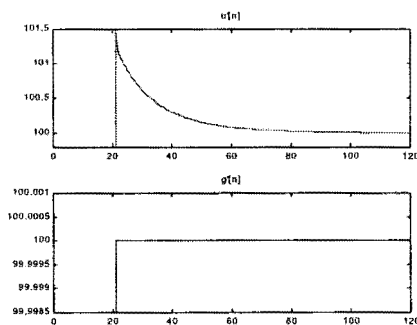
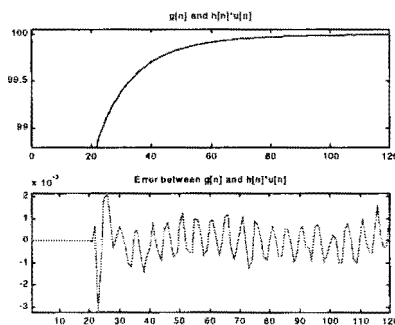
- Y-axis:

The order of  $B(q)$  is four, the order of  $F(q)$  is three.



- Z-axis:

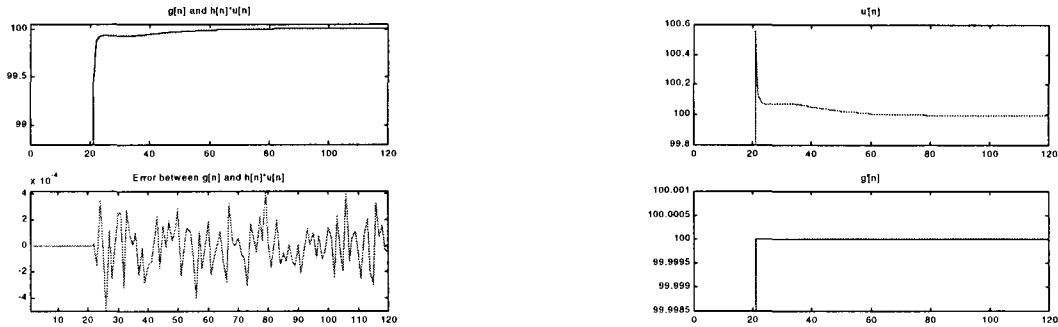
The order of  $B(q)$  is four, the order of  $F(q)$  is three.



# Appendix C : Simulation Results of the Box Jenkins Model

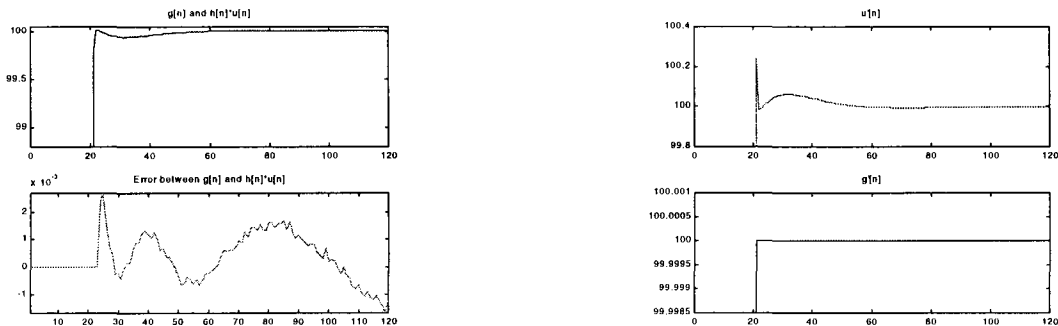
- X-axis:

The order of  $B(q)$  is five, the order of  $F(q)$  is four.



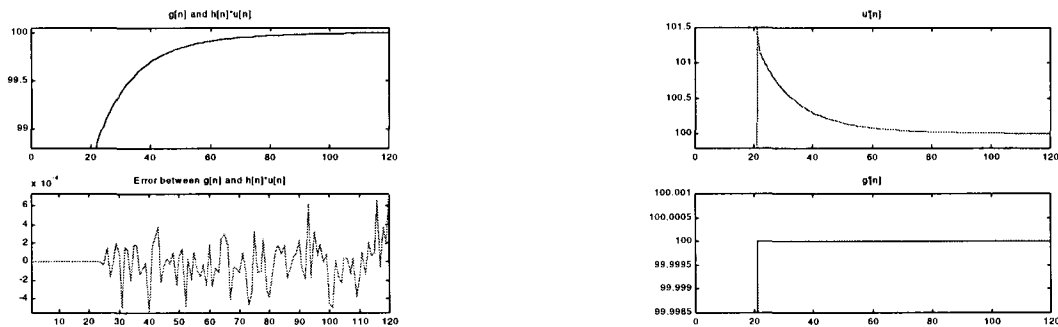
- Y-axis:

The order of  $B(q)$  is four, the order of  $F(q)$  is three.



- Z-axis:

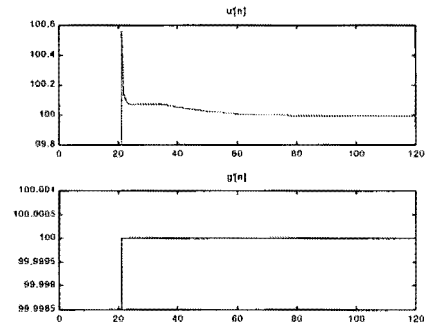
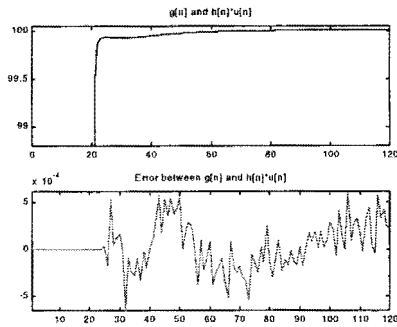
The order of  $B(q)$  is eight the order of  $F(q)$  is seven.



# Appendix D : Simulation Results of the ARMAX model

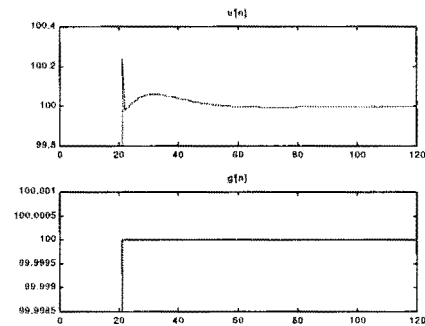
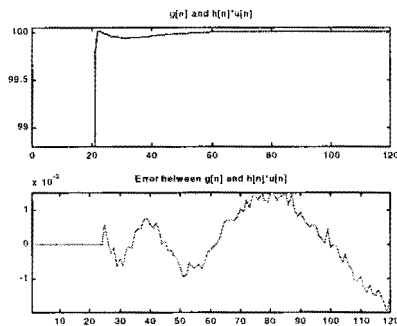
• X-axis:

The order of  $A(q)$  is four, the order of  $B(q)$  is five.



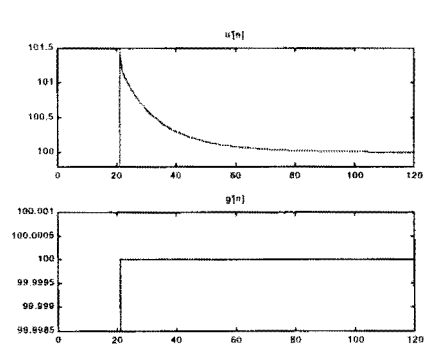
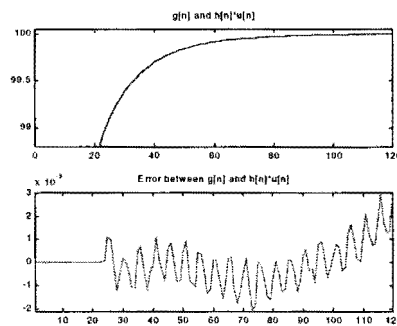
• Y-axis:

The order of  $A(q)$  is four, the order of  $B(q)$  is five.



• Z-axis:

The order of  $A(q)$  is four the order of  $B(q)$  is five.



---

# Bibliography

---

- [PHI] Philips Medical Systems  
BASIC PRINCIPLES OF MR IMAGING  
Second Edition
- [MOR88] Morich, M.A. and D.A. Lampman, W.R. Dannels, F.T.D. Goldie  
EXACT TEMPORAL EDDY CURRENT COMPENSATION IN MAGNETIC  
RESONANCE IMAGING SYSTEMS.  
IEEE Trans. Med. Imag., Vol.7 (1988) No. 3, p.247-256
- [FRY97] Fry, M.E. and S. Pittard, I.R. Summers, W. Vennart, F.T.D. Goldie  
A PROGRAMMABLE EDDY CURRENT COMPENSATION SYSTEM FOR MRI  
AND LOCALISED SPECTROSCOPY  
J. Magn. Reson. Imag. Vol. 7 (1997), p.455-458
- [JEH90] Jehenson, P. and M. Westphal, N. Schuff  
ANALYTICAL METHOD FOR THE COMPENSATION OF EDDY-CURRENT  
EFFECTS INDUCED BY PULSED MAGNETIC FIELD GRADIENTS IN NMR  
SYSTEMS  
J. Magn. Reson., Vol. 90 (1990), p.264-278
- [VAA90] Vaals, J.J. van and A.H. Bergman  
OPTIMISATION OF EDDY CURRENT COMPENSATION  
J. Magn. Reson., Vol. 90 (1990), p.52-70
- [PRE89] William H. Press, Brian P. Flannery, Saul A. Teukolsky ... [et al.].  
NUMERICAL RECIPES IN PASCAL : THE ART OF SCIENTIFIC COMPUTING  
Cambridge: Cambridge University Press, 1989
- [MOR88] Morich, M.A. and D.A. Lampman, W.R. Dannels, F.T.D. Goldie  
EXACT TEMPORAL EDDY CURRENT COMPENSATION IN MAGNETIC  
RESONANCE IMAGING SYSTEMS.  
IEEE Trans. Med. Imag., Vol.7 (1988) No. 3, p.247-256
- [BOS94] Bosch, P.P.J. van den and A.C. van der Klauw  
MODELING, IDENTIFICATION AND SIMULATION OF DYNAMICAL SYSTEMS  
Florida: CRC Press, 1994
- [ZHU93] Zhu, Y and T. Backx  
IDENTIFICATION OF MULTIVARIABLE INDUSTRIAL PROCESSES FOR  
SIMULATION, DIAGNOSIS AND CONTROL  
London: Springer-Verlag, 1993

- [STE65] Steiglitz, K. and L.E. McBride  
A TECHNIQUE FOR THE IDENTIFICATION OF LINEAR SYSTEMS  
IEEE Trans. Automat. Control, Vol. 10 (1965), p. 461-464
- [STO81] Stoica, P. and Torsten Söderström  
THE STEIGLITZ-MCBRIDE IDENTIFICATION ALGORITHM REVISITED –  
CONVERGENCE ANALYSIS AND ACCURACY ASPECTS  
IEEE Trans. Automat. Control, Vol. 26 (1981), No. 3, p. 712-717